E&G Quaternary Sci. J., 71, 59–81, 2022
https://doi.org/10.5194/egqsj-71-59-2022

Open Access E&G Quaternary Science Journal

Research article

Chronostratigraphic and geomorphologic challenges of last glacial loess in Poland in the light of new luminescence ages

Ludwig Zöller[1,2], Manfred Fischer[1], Zdzisław Jary[3], Pierre Antoine[4], and Marcin Krawczyk[3]

[1]Geomorphology Chair, University of Bayreuth, 95440 Bayreuth, Germany
[2]BayCEER, University of Bayreuth, 95440 Bayreuth, Germany
[3]Institute of Geography and Regional Development, Faculty of Earth Sciences and Environmental Management, University of Wrocław, ul. Cybulskiego 34 (2nd floor), 50-205 Wrocław, Poland
[4]Laboratoire de Géographie Physique, Environnements Quaternaires et Actuels, CNRS, 1 Pl. A. Briand, 92195 Meudon CEDEX, France

Correspondence: Ludwig Zöller (ludwig.zoeller@uni-bayreuth.de)

Relevant dates: Received: 16 February 2021 – Revised: 29 January 2022 – Accepted: 23 February 2022 – Published: 1 April 2022

How to cite: Zöller, L., Fischer, M., Jary, Z., Antoine, P., and Krawczyk, M.: Chronostratigraphic and geomorphologic challenges of last glacial loess in Poland in the light of new luminescence ages, E&G Quaternary Sci. J., 71, 59–81, https://doi.org/10.5194/egqsj-71-59-2022, 2022.

Abstract: The aim of this study is to check the validity of luminescence ages obtained from last glacial–interglacial Polish loess palaeosol sequences (LPSs) by several established current protocols, with respect to sound geomorphological and chronostratigraphic interpretations. We report 38 new optically stimulated luminescence (OSL) ages from fine-grained (4–11 µm) quartz separates extracted from four loess palaeosol sequences in Poland, measured in the Bayreuth Luminescence Laboratory, Germany. The investigated sections are situated in Lower Silesia in the southwest (Zaprężyn, Trzebnica Hills, and Biały Kościół, Strzelin Hills), the Sandomierz Upland (Złota) in central Poland, and the Volhynian Upland (Tyszowce) in the east, allowing for regional comparison. From one Silesian section (Biały Kościół) 12 new post-infrared infrared stimulated luminescence (pIRIR) ages are presented in addition to the quartz ages of identical sample material. The obtained ages are compared to already published independently elaborated middle-grain (45–63 µm) and coarse-grain (90–125 µm) quartz ages and pIRIR ages from fine grains produced in the Gliwice Luminescence Laboratory (Poland). This comparison shows that in many cases the middle- and coarse-grain quartz ages underestimate the fine-grain quartz ages, but a general rule has not been able to be established so far, likely due to different geological origin of the quartz grains. Even fine-grain quartz ages $\geq\sim 50$ ka may be underestimated with respect to lithostratigraphic expectations. For pIRIR ages, however, no evidence for age underestimates has been found in the studied sections, but they are more easily prone to age overestimates due to unknown residual doses at deposition in a periglacial environment.

Basic agreement between the luminescence-based chronologies elaborated in the two involved laboratories can be stated for the first time in contrast to other previous studies. The observed age differences are, however, critical for the accurate time bracketing of geomorphologic and pedostratigraphic features such as ice wedging, thermokarst erosion events, and interstadial soil formations and for their attribution to marine isotope stages. Alternative interpretations are discussed including possible periglacial mirroring of pre-LGM ice advances (Ristinge and Klintholm advances) in the southwestern

Baltic Sea area. The uncertainty in luminescence ages from pre-Holocene loess due to fossil ice during permafrost conditions is the major systematic error source which will be addressed but at present is far from an unambiguous solution. The present study focuses on a complex of interstadial soils now labelled L1SS1 and on harsh periglacial climate afterwards and before, yielding some unexpected results for the timing of ice wedging and thermokarst processes. In order not to leave the users alone with the decision about the most credible dating, the suggested way forwards is to simultaneously apply various luminescence dating protocols including different quartz grain sizes and pIRIR from fine polymineral grains, as an honest approach to reliable time bracketing of geomorphological processes and stratigraphic events under debate. A refinement of this approach remains challenging as far as the sole reliable dating protocol is not ensured.

Kurzfassung:

Das Ziel dieser Studie ist die Überprüfung der Aussagekraft von Lumineszenzaltern aus Löss-Paläoboden-Sequenzen (LPS) des letzten Glazial-Interglazialzyklus in Polen, welche durch verschiedene etablierte aktuelle Protokolle erzielt wurden, unter Berücksichtigung gut fundierter geomorphologischer und chronostratigraphischer Interpretationen. Wir präsentieren 38 neue OSL-Alter von feinkörnigen (4–11 µm) Quarz-Separaten aus vier LPS in Polen, die im Lumineszenzlabor in Bayreuth (Deutschland) gemessen wurden. Die untersuchten Profile liegen in Niederschlesien (Zaprężyn, Trzebnica Hügelland und Biały Kościół, Strzelin Hügelland), im Sandomierz Oberland (Złota), und im Wolhynischen Oberland (Tyszowce) im Osten, wodurch auch regionale Vergleiche ermöglicht werden. Von einem schlesischen Profil (Biały Kościół) werden zusätzlich zu den Quarz-Altern 12 neue pIRIR-Alter vom identischen Probenmaterial mitgeteilt. Die erzielten neuen Alter werden mit bereits publizierten unabhängig erarbeiteten Quarz-Mittelkorn- (45–63 µm) und Quarz-Grobkorn- (90–125 µm) Altern aus dem Lumineszenz-Labor in Gliwice (Polen) verglichen. Dieser Vergleich zeigt, dass in vielen Fällen die Mittelkorn- und Grobkorn-Quarzalter die Feinkorn-Quarzalter unterschätzen. Aber eine generelle Regel kann noch nicht erstellt werden, vermutlich aufgrund unterschiedlicher geologischer Herkunft der Quarzkörner. Selbst Quarz-Feinkornalter $\geq\sim 50$ ka können in Bezug auf lithostratigraphische Erwartungen unterschätzt sein. Für pIRIR-Alter wurden jedoch in den untersuchten Profilen keine Hinweise auf Unterschätzung gefunden, sie sind hingegen eher anfällig für Altersüberschätzungen aufgrund unbekannter Residual-Dosen (Restalter) bei Ablagerung in einem periglazialen Milieu.

Grundsätzliche Übereinstimmung zwischen den Lumineszenz-basierten Chronologien aus den beiden involvierten Laboratorien kann erstmals – im Gegensatz zu früheren anderen Studien – festgestellt werden. Die beobachteten Altersunterschiede erweisen sich jedoch als kritisch für eine exakte zeitliche Eingrenzung geomorphologischer und pedostratigraphischer Merkmale wie Eiskeilbildungen, Thermokarst-Erosionsereignisse und interstadiale Bodenbildungen sowie deren Zuordnung zu Marinen Isotopen-Stadien. Alternative Interpretationen werden diskutiert einschließlich periglazialer Spiegelung von Prä-LGM-Eisvorstößen (Ristinge und Klintholm-Vorstöße) im Gebiet der südwestlichen Ostsee. Die Unsicherheit von Lumineszenz-Altern aus prä-Holozänem Löss aufgrund fossilen Bodeneises während periglazialer Verhältnisse stellt die bedeutendste systematische Fehlerquelle dar, die näher angesprochen wird aber noch weit von einer unzweideutigen Lösung entfernt ist. Die vorliegende Studie fokussiert auf einen Komplex von Interstadialböden, der jetzt als L1SS1 bezeichnet wird, sowie auf harsche periglaziale Klimabedingungen davor und danach, und führt zu einigen unerwarteten Ergebnissen für die Zeitstellung von Eiskeilbildungen und Thermokarst-Prozessen. Um die Anwender nicht alleine zu lassen mit der Entscheidung über die glaubwürdigste Datierung wird für den Weg vorwärts vorgeschlagen, simultan verschiedene Lumineszenzdatierungs-Protokolle anzuwenden einschließlich unterschiedlicher Quarz-Korngrößen und pIRIR an der polymineralischen Feinkornfraktion. Dieser Weg stellt den aufrichtigen Versuch dar, eine verlässliche zeitliche Eingrenzung in Frage stehender geomorphologischer Prozesse und stratigraphischer Ereignisse vorzunehmen. Eine Verfeinerung dieses Ansatzes bleibt eine Herausforderung solange ein einzig verlässliches Datierungsprotokoll nicht abgesichert ist.

1 Introduction

The European loess belt, extending from northern France to the Caspian Lowland (Haase et al., 2007; Antoine, 2013), is split into a northern and a southern branch by the Central European Uplands and the Carpathian Mountains. Whereas a largely conclusive and elaborate chronostratigraphy of loess palaeosol sequences (LPSs) for the last interglacial–glacial cycle was already available for the southern branch and the western part of the northern branch (Antoine et al., 2015; Fuchs et al., 2013; Moine et al., 2017; Rousseau et al., 2017), gaps of knowledge concerning the chronology persisted for the rest of the northern branch, in particular for areas east of the Rhine. The international workshop "Closing the gap – North Carpathian loess traverse in the Eurasian loess belt" held in Wrocław, Poland, in 2011 (Jary, 2011) brought together loess experts from many European countries and from the USA. It aimed at addressing pending problems in European loess chronostratigraphy. Due to the proximity to the maximum extent of the last glacial Scandinavian Ice Sheet (SIS), the northern branch is expected to be best suited for investigating the impact of temporal SIS dynamics on lithostratigraphic and pedostratigraphic characteristic features of LPSs off the ice margin. Considering the differentiation between the global LGM and regional LGM (Hughes et al., 2013) as well as the ice dynamics in the SW sector of the SIS (Lüthgens et al., 2020), a premature correlation with marine isotope stages (MISs) should be set aside to avoid jumping to conclusions.

Last glacial loess in southwestern Poland (Silesia) was deposited closer to the maximum ice advance of the Scandinavian Ice Sheet (SIS) than in the eastern part of Poland. The Odra ice lobe in particular reached quite far south in the German state of Brandenburg (Brandenburg stage) and in western Poland (Leszno stage; see Marks, 2005, 2011). Even if there is now luminescence dating evidence that the regional last glacial maximum (R-LGM; cf. Hughes et al., 2013) predates the global LGM by several thousand years (Lüthgens and Böse, 2011; Hardt et al., 2016), it can be expected that witnesses of harsh periglacial climate such as ice wedge networks are more probably found in ice-proximal than in distal loess. This instance is of special interest and advantageous for geomorphology, palaeoclimatology and loess stratigraphy. A disadvantage, however, is the fact that brutal collapse of ice wedge networks linked to permafrost decay (Murton, 2001) induces intense thermokarst erosion events in loess sequences (Antoine, 2013; Antoine et al., 2014). Such processes, already evidenced for the northern loess belt branch in western European LPSs (Antoine et al., 2015), lead to major erosional unconformities and, thus, to stratigraphic gaps, easily causing misinterpretations of the timing of those processes. Similar periglacial features are to be expected in Polish loess and will be one focus of this contribution.

Thermoluminescence (TL) and optically stimulated luminescence (OSL) dating have been widely applied to loess in Poland since the work by Butrym and Maruszczak (1983). At the end of the last century TL loess chronostratigraphy in Poland was well correlated with the marine record (Maruszczak, 1991, 2001), but these results have often been inconsistent with OSL ages (see review by Moska and Bluszcz, 2013). Luminescence dating methods applied to sediments are based on the accumulation of ionizing radiation damage in mineral grains after the last resetting of the latent (inherent) signal. In sediments resetting occurs by exposure to daylight (e.g. Preusser et al., 2008). Sources of error in luminescence dating are manifold, but before they can – perhaps – be eliminated, they must be detected and addressed. The main systematical error sources for sediments include incomplete resetting at deposition and the approximation of a representative past water content since burial.

Furthermore, redeposition of loess beds by gelifluction lobes (and also hillwash processes) in periglacial environments poses a major problem for luminescence dating, as geliflucted material consists of a mixture of optically reset (bleached) and unbleached components or even completely unbleached older loess-like sediments (Zöller, 1989). In narrow sections, the unconformities of such beds are often hard to detect and easily cause misinterpretations. Radiocarbon dating of buried organic material may also suffer from such problems, besides other complications affecting radiocarbon dating of loess beds, for example, post-burial C-isotope exchange (e.g. Gocke et al., 2010; Scheidt et al., 2021). In this contribution we present new optical dating results from important loess sections in Poland.

For stratigraphic orientation we use the system recently proposed for last glacial Polish loess by Jary and Ciszek (2013) and later modified by Marković et al. (2015), discriminating between four major units within the last interglacial–glacial cycle (from bottom to top, with S for soil, L for loess, and L1SS1 denoting the interstadial soil complex): S1, L1LL2, L1SS1, and L1LL1. Most of the sections worked on here have already been dated by Piotr Moska (Gliwice) in the past few years. Some problems were, however, found, among them an apparent grain size dependency of ages obtained from quartz grains (coarse silt and sand fractions). In the Bayreuth Luminescence Laboratory, only the fine-grain fraction (4–11 µm) was used for dating, following experiences by Kreutzer et al. (2012). The dating results will be compared, and divergences beyond 1σ errors will be discussed in view of the ages expected from lithostratigraphy.

We present optical dating results (OSL from quartz grains, post-infrared infrared stimulated luminescence (pIRIR) from fine polymineral grains) originating from LPSs in Silesia (Biały Kościół in the Strzelin Hills south of Wrocław, Zaprężyn, in the Trzebnica Hills north of Wrocław), Złota near Sandomierz and the river Vistula (Wisła), and Tyszowce in the Volhynian Upland southeast of Lublin (Fig. 1). The spatial context of the investigated sites and the ice advances of the last glacial (Vistulian) SIS can be seen in Fig. 2. With the exception of the Zaprężyn site, luminescence dating results ob-

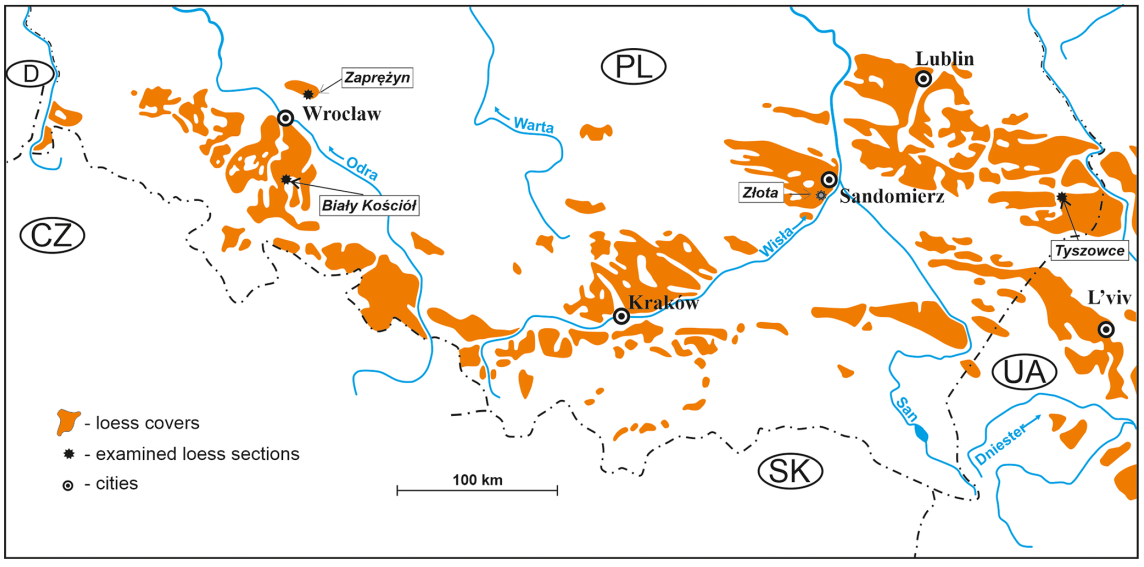

Figure 1. Loess map of Poland, with locations of investigated sites framed by black rectangles (from Jary et al., 2011, modified).

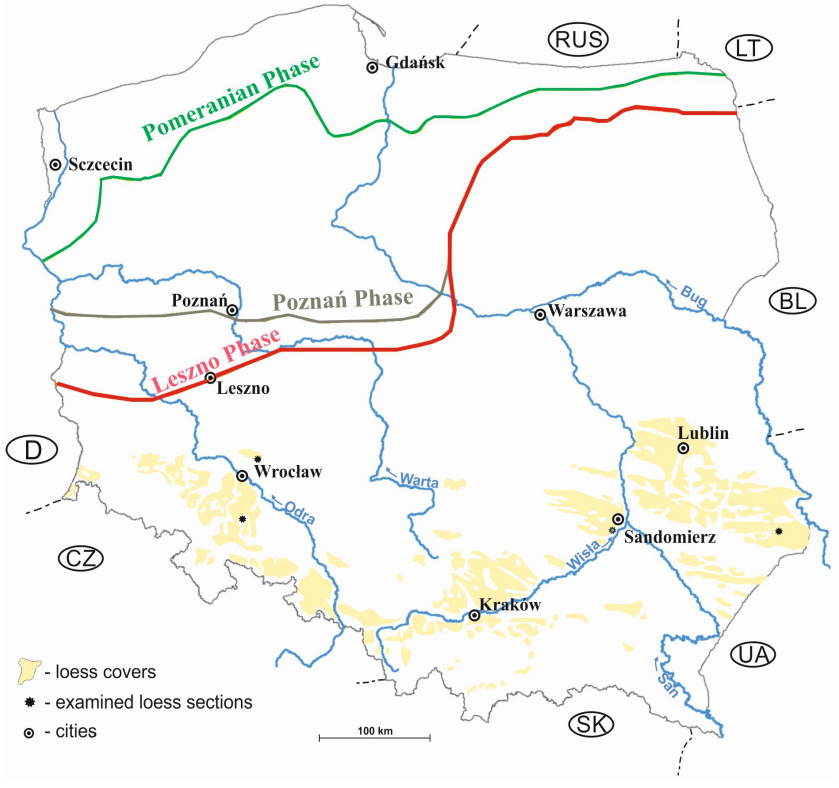

Figure 2. Limits of the major glacial phases during the Late Vistulian in Poland and spatial context of the loess belt.

tained in Gliwice have been published in recent years (Moska et al., 2011, 2012, 2015, 2017, 2018, 2019) including detailed site descriptions, whereas the ages obtained in Bayreuth have not been published so far. It should be noted that the two luminescence laboratories did not work on identical shared sample material, but with the exception of the lower part of the Tyszowce site, the sampling points could be correlated well, based on the lithostratigraphic subdivisions. Nevertheless, the present study offers a good opportunity to jointly compare and discuss luminescence dating results obtained in different laboratories.

2 Material and methods – luminescence dating

This contribution deals with chronostratigraphic problems and palaeoclimate-triggered geomorphological site formation of the investigated sites with loess exposures. Numerous other investigations have been carried out into lithostratigraphy, grain size variations, periglacial features, and geochemistry, which can be mentioned only briefly here with the relevant literature. Some radiocarbon ages are also mentioned but without further going into details of their reliability and specific problems.

Instead, this study deals mainly with the application of various established luminescence dating techniques. First of all, OSL dating of quartz is presented because feldspars are often affected by so-called anomalous fading of their luminescence signal, resulting in age underestimation (Preusser et al., 2008). Whereas the Gliwice laboratory has executed OSL dating mainly of middle-grain (45–63 µm) but also coarse-grain (90–125 µm) quartz separates, the Bayreuth laboratory contributes OSL fine-grain quartz ages, both laboratories using the single-aliquot regeneration (SAR) method (Murray and Wintle, 2000). The rather low natural dose saturation level of quartz OSL, however, limits the dating range of loess to ca. 100 ka or less. It was demonstrated that the post-infrared infrared stimulated luminescence (pIRIR) method can reduce anomalous fading significantly and, thus, extend the age range of IRSL dating far beyond the saturation limit of quartz (Thiel et al., 2011; Murray et al., 2013). Therefore, testing this method on the fine-grain feldspar-bearing fraction of Polish loess is recommendable.

2.1 Sampling and sample processing

Both involved laboratories use a very similar sampling procedure for unconsolidated rocks such as loess. A steel tube with an inner diameter of 40 mm (Gliwice) or more (50 to 60 mm, Bayreuth) is hammered horizontally into a well-cleaned vertical part of the exposure. After pulling or digging out the filled cylinder under shadow, both ends are immediately sealed with light-tight caps and taped. Additional material is taken from the hole for dosimetry and moisture measurements and sealed in airtight plastic bags. Some samples of more condensed layers for the Bayreuth laboratory were, however, cut as blocks with ca. 10 cm length edges and wrapped to be light-tight.

In the dark laboratory under subdued red light (in the Bayreuth laboratory 640 ± 42 nm; no wavelengths are given for the Gliwice laboratory) the cylinders and the blocks were opened and the outer 1 to 2 cm thick rims which may have seen some light during sampling were removed. It was thus assured that only material completely unexposed to daylight during sampling was processed for luminescence measurements. In the Bayreuth laboratory the removed sediment was later used for thick-source alpha counting (TSAC, for U and Th contents) and for ICP-OES (for K content) because it was situated closest to the further-processed sample material.

Further sample processing (sieving, chemical pretreatment, grain size separation, mineral separation) was handled slightly different in both laboratories, which did not affect, however, the aim to receive well-defined grain size classes and mineral separates. The procedures executed in the Gliwice laboratory are mentioned in the cited publications, for example, in Moska et al. (2015); those applied in the Bayreuth laboratory are described, for example, in Fuchs et al. (2013) or in Zöller et al. (2014). In Bayreuth unlike in Gliwice the fine-grain quartz fraction (4–11 µm) was measured by OSL and much attention had to be given to obtain pure quartz in this fraction by etching it for a minimum of 7 d in hydrofluoric acid (H_2SiF_6). The purity of the quartz enrichment was checked by IRSL measurements.

2.2 Luminescence measurements and data processing in the Bayreuth laboratory

OSL measurements to determine the equivalent dose (D_e) of fine-grain quartz separates were carried out on two Risø TL/OSL DA-15 readers, equipped with blue LEDs (470 ± 30 nm) for stimulation; a Thorn EMI 9235 QA photomultiplier combined with a Hoya U340 7.5 mm filter (290–370 nm) for detection; and a $^{90}Sr/^{90}Y$ β source (0.75 and 1.48 GBq, respectively) for irradiation, delivering a dose rate of 2.72 Gy min^{-1} to fine grains on aluminium discs for the Risø reader with the 0.75 GBq β source and 9.14 Gy min^{-1} for the Risø reader with the 1.48 GBq β source (reference date August 2010; cf. Fuchs et al., 2013, recalculated for the respective date of irradiation using the decay constant of ^{90}Sr). OSL decay curves were measured for 40 s at elevated temperatures (125 °C), using a cut heat for the test dose of 220 °C (same as preheat). Based on dose recovery and preheat plateau tests, a preheat temperature of 220 °C was chosen for the natural and regenerated OSL signals. For further processing OSL signals were integrated from the first 0.6 s of the decay curve minus a background averaged from the last 7.5 s.

For IRSL measurements the same readers were used but with infrared LEDs (850 nm – main peak) for stimulation and a 3 mm Chroma Technology D410/30× interference filter, restricting the detection window to the blue-violet wavelength band. For the fine-grain polymineral fraction of 12 samples from the new profile at Biały Kościół (2018), we used the $pIRIR_{290}$ protocol adopted from Murray et al. (2013; see Table 1). The first 0.6 s (first six channels) of the shine-down curves was evaluated for D_e determinations, and the segments from 150 to 200 s were used as background. Differently from Moska et al. (2019) no subtraction of an experimentally approximated residual background dose was executed (cf. Murray et al., 2013). The sequences are summarized in Table 1.

Table 1. Sequence of $pIRIR_{290}$ (left) and OSL (right) measurements.

pIRIR			Quartz OSL		
Step	Treatment	Observed	Step	Treatment	Observed
1	Dose		1	Dose	
2	Preheat, 60 s at 320 °C		2	Preheat, 10 s at 220 °C	
3	IR stimulation, 200 s at 50 °C	Lx	3	OSL, 40 s at 125 °C	Lx
4	IR stimulation, 200 s at 290 °C	Lx	4	Test dose	
5	Test dose		5	Cut heat to 220 °C	
6	Preheat, 60 s at 320 °C		6	OSL, 40 s at 125 °C	Tx
7	IR stimulation, 200 s at 50 °C	Tx	7	Return to step 1	
8	IR stimulation, 200 s at 290 °C	Tx			
9	Return to step 1				

The program Analyst version 4.31.9 (Duller, 2015) was used for processing and evaluation of OSL and IRSL data. Regenerated growth curves were fitted to a single exponential saturation function. Plots of OSL decay curves and regenerated growth curves for three samples (fine quartz grains) from the Biały Kościół section (BT 1672, BT 1673, and BT 1675) are shown in Fig. S4 in the Supplement, and a plot with preheat plateau test and recuperation for BT 1675 is shown in Fig. S5.

2.3 Dosimetry

U and Th concentrations were calculated from thick-source alpha counting (TSAC) after powdering following Zöller and Pernicka (1989) and after sealing the sample holders for a minimum of 3 weeks. A Littlemore TSAC system 7287 with three photomultiplier heads standing in a dark quasi-thermoconstant cellar room was used. Total counts reached a minimum of ca. 4000 events including slow and fast pair counts, allowing for ca. 10 % accuracy of calculated U and Th concentrations. Secular equilibrium of the U and Th decay chains was assumed for the samples consisting of loess or loess-derived sediments. The TONY standard (Zöller and Pernicka, 1989) was counted regularly in all three photomultiplier heads and was always found to be within ±3 % of the default count rate.

K concentrations were measured by ICP-OES in the BayCEER central laboratory at the University of Bayreuth. In the Gliwice laboratory high-resolution gamma spectrometry (HPGe detector) was used for determining activities of U and Th decay chains and ^{40}K, and conversion factors to the dose rate were by Guérin et al. (2011). Due to the large dry sample mass of 800 g (Marinelli beaker geometry), gamma emissions at very low energies are not resolved with an accuracy necessary to detect radioactive disequilibrium.

2.4 Age calculation

Luminescence ages were calculated using the program ADELE v2015 021a beta which was a test version of the recently released ADELE v2017 (Degering and Degering, 2020). It includes calculation of cosmic dose rates and dose conversion rates updated by Guérin et al. (2011). The determination of the alpha-efficiency factor (a value) for fine grains is unjustifiably consuming machine time. Therefore, a values for larger sets of Pleistocene samples are increasingly adopted from the literature with rather wide error bars. An a value of 0.035 ± 0.005 was taken for the OSL of fine-grain quartz samples (Lai et al., 2008) and 0.1 ± 0.01 for the $pIRIR_{290}$ of fine-grain samples (cf. Kreutzer et al., 2014, for $pIRIR_{225}$), but $pIRIR_{290}$ ages were also calculated with 0.085 ± 0.01 (cf. Schmidt et al., 2018). We decide, however, in favour of the a value of 0.1 ± 0.01 for the time being over the suggestion of Schmidt et al. (2018) (see below in Sect. 3, Results).

Moisture contents ranging between 11 % and 23 % were taken from measurements of bags sealed in the field as far as the wet unit weight could be dug up; otherwise 15 ± 5 % was inserted. Moisture contents used for age calculation are also listed in Table S1 in the Supplement. Higher soil moisture absorbs more of the energy of ionizing irradiation than low soil moisture, which is strongest for alpha particles, less for beta radiation, and even less for gamma radiation (Aitken, 1998). A lower moisture content used in the age equation will therefore yield a lower apparent age and vice versa. The problem of representative past moisture content needs a critical evaluation for two reasons. Pleistocene loess was deposited under climatic and environmental conditions quite different from Holocene ones. The climate during loess formation in central Europe was most of the time dryer and cooler than at present with an impact on mean annual to centennial soil moisture. Overall lower precipitation may, however, at least partially been counterbalanced by lower evapotranspiration. Furthermore, the last glacial–interglacial cycle experienced a number of climatic fluctuations at a periodicity comparable to Dansgaard–Oeschger cycles or even faster (Rousseau et al., 2017; Moine et al., 2017). The greatest problem concerning past soil moisture is posed by occurrence of permafrost, which can produce ice lensing and, thus, water and/or ice

oversaturation at a micro-scale to local scale for tens to several thousands of years in the research area (probably longer in higher latitudes). With respect to the diameter of the sampling tubes, ice lensing on a millimetre scale is not as severe as the formation of tabular ice many centimetres to decimetres thick, and most problematic are thick ice wedges. Even if the persistence of ice lenses and wedges may have lasted only a few per cent to 10 % of the total time span covering the last glacial cycle, the impact on water/ice content of the ground due to oversaturation may not be negligible. But the effect on the dose rate and, thus, on the luminescence age cannot be quantified; it can only be estimated to the best of one's knowledge. For this reason it is honest to assume higher-than-usual error limits for moisture content in the error calculation of a luminescence age. Soil scientists and palaeopedologists can give helpful advice to set limits for minimum and maximum water saturation of loess soils in the field. Systematic OSL dating studies in loess areas with actual permafrost, for example, Alaska or Siberia, may be a propellant to a better understanding of the problem.

3 Results

For all of the four LPS sections the new luminescence ages from the Bayreuth laboratory will be presented first. Analytical data and ages are given in Table S1. Obtained ages are then compared with already-available ages from the Gliwice laboratory, except for the Zaprężyn section (OSL ages not yet published).

3.1 The Silesian key section – Biały Kościół

The loess section is located near the village of Biały Kościół, on the western slope of the Oława valley (50°43′38.73″ N, 17°01′ 29.57″ E) at about 180 m a.s.l. Already in 2014 three test samples for the Bayreuth laboratory (BT 1482, BT 1483, and BT 1484 – violet in Fig. 3) were taken by Ludwig Zöller and Zdzisław Jary at a depth between ca. 4.4 and 5.7 m from the older exploratory excavation (2009), from which the samples for the Gliwice laboratory had also been taken some years before, but those three samples will not be further discussed. As this dig was severely endangered by collapses, a new dig was created by Zdzisław Jary and his team in 2017 and 2018, 6 m aside from the older one. Lithostratigraphic units could be followed from the older to the new dig; the "upper younger loess" L1LL1 is, however, a few decimetres thicker in the new dig. For optical dating between 3.7 and 9.5 m depth of the new section, 12 samples were extracted in June 2018.

Litho- and pedostratigraphic units are described in detail in Moska et al. (2019) together with physical and chemical soil properties. Dating results from fine quartz grains (OSL) and from fine polymineral grains ($pIRIR_{290}$) obtained in Bayreuth are shown in Fig. 3 (with an age–depth plot; see also Fig. S3); those obtained in Gliwice are shown in Fig. 4. Analytical results for the samples dated in Bayreuth are given in Table S1.

Quartz ages (4–11 µm) from Bayreuth are in stratigraphic order within their 1σ uncertainties. An arrangement in groups is obvious: (i) from L1LL1 (BT 1679) to the upper part of L1SS1 ranging from ca. 25 to ca. 35 ka, (ii) the L1SS1 lower brownish part and L1LL2 around ca. 60 ka, (iii) the upper part of the S1 complex at ca. 75 ka, and (iv) the lower part of the S1 complex at 112 ± 8.6 ka (Figs. 3 and S3 left).

Fine-grain polymineral ages ($pIRIR_{290}$) obtained in Bayreuth (PM) were calculated with an a value of 0.1 ± 0.01 since evidence for a positive correlation between the IRSL stimulation temperature and height of the a value was observed (Kreutzer et al., 2014). The complex of problems when using a common a value was, however, outlined by Schmidt et al. (2018). Following their suggestion the $pIRIR_{290}$ ages were recalculated using 0.085 ± 0.01, resulting in 4 % to 5 % higher ages, but so far there has been no proof of the trueness of this value, and the a-value determinations of Kreutzer et al. (2014) predominantly originate from Saxonian loess in the proximity of Lower Silesia. Therefore, in Fig. 3 only the $pIRIR_{290}$ ages for $a = 0.1$ are plotted. But for both a values, calculated ages are listed in Table S1. The $pIRIR_{290}$ ages are in stratigraphic order within their 1σ uncertainties, and for samples extracted from the L1LL1 loess (BT 1677 to BT 1679), they agree within error bars with the quartz ages. But from samples taken within the L1SS1 palaeosol or deeper $pIRIR_{290}$ ages are significantly older than the quartz ages. For sample BT 1676 the significant overestimate of the $pIRIR_{290}$ age (40.2 ± 3.4 ka) referred to the quartz age (28.0 ± 1.8 ka) is most likely due to incomplete bleaching of $pIRIR_{290}$ because this sample originates from reworked L1SS1 material, as is visualized in Fig. 3. An arrangement in groups is obvious (Figs. 3b and S3 right): (i) L1LL1 to L1SS1 from ca. 27 to ca. 45 ka, (ii) the L1SS1 lower brownish part and L1LL2 at ca. 70 ka, (iii) the upper part of the S1 complex at ca. 100 ka, and (iv) the lower part of the S1 complex at > 300 ka. Although the apparent $pIRIR_{290}$ age of the lowermost sample BT 1668 needs to be verified (because of dose saturation, only 4 of 15 aliquots were suitable, and also due to possible dose overestimation described by Avram et al., 2020), it points to a very long hiatus within the S1 complex. IRSL decay curves and a dose–response curve of a suitable aliquot are shown in Fig. S6. Another but not so long-lasting hiatus is apparent within the grey and the brownish part of L1SS1 from both fine-grain quartz and fine-grain polymineral ages. L1SS1 as characterized in Moska et al. (2019) appears therefore as a pedocomplex or a complex like in Saxonian loess (cf. Meszner et al., 2013). This ca. 25 kyr long hiatus within L1SS1 is also apparent from the $pIRIR_{290}$ ages.

Ages obtained by the $pIRIR_{290}$ protocol become significantly older than quartz ages from sample BT 1676 (top of L1SS1) downwards. This systematic behaviour of ages can hardly be explained by assuming a sudden increase in resid-

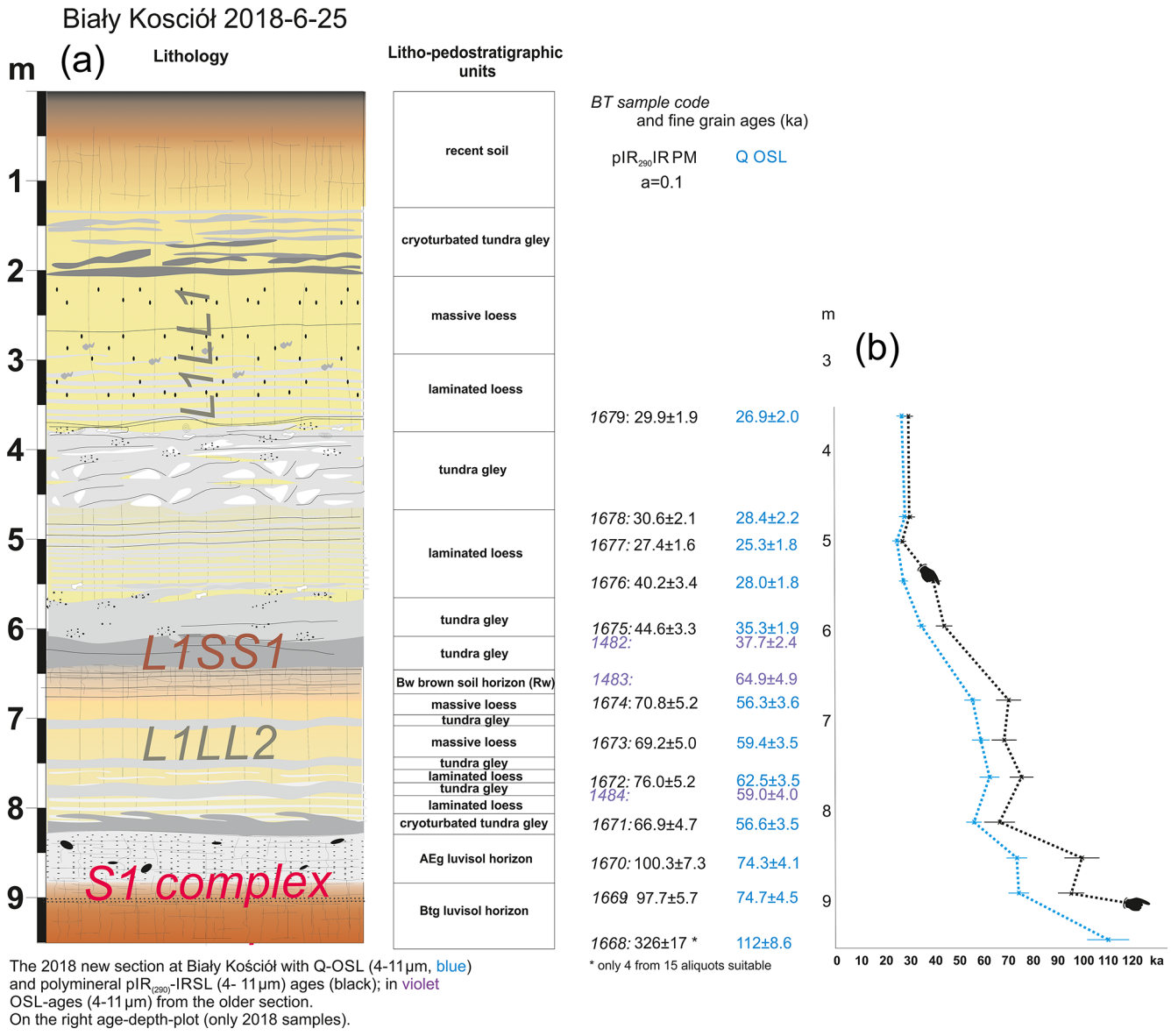

The 2018 new section at Biały Kościół with Q-OSL (4-11 µm, blue) and polymineral pIR$_{(290)}$-IRSL (4- 11 µm) ages (black); in violet OSL-ages (4-11 µm) from the older section.
On the right age-depth-plot (only 2018 samples).

Figure 3. **(a)** OSL ages from fine quartz grains and pIRIR$_{290}$ ages from fine polymineral grains obtained from the Biały Kościół section (2018) in the Bayreuth laboratory. Litho-pedostratigraphic units (legend) are by Marcin Krawczyk. **(b)** Age–depth plot of fine-grain quartz ages (blue) and pIRIR$_{290}$ ages from fine polymineral grains (black) obtained from the Biały Kościół section (2018) in the Bayreuth laboratory. Only samples from the 2018 section are regarded. The unconfident apparent pIRIR$_{290}$ age of BT 1688 is off the scale (hand to the right). Note the bulge of the pIRIR$_{290}$ plot below ca. 5.5 m depth (hand downwards) and sample BT 1671 at ca. 8.2 m. The quartz plot betokens this bulk less distinctly.

ual doses at deposition, even if the slightly higher pIRIR$_{290}$ ages referred to the quartz ages in the higher part of the section may be a sign of a residual dose in the range of some 10 to 15 Gy.

Dating results published by Moska et al. (2019) are presented from the coarse-grain quartz fraction (90–125 µm), the middle-grain quartz fraction (45–63 µm), and the fine-grain polymineral fraction (4–11 µm). Ages from the coarse-grain fraction show some stratigraphic inconsistencies (samples BK18, BK13, and BK8) which is not the case for the finer fractions within uncertainties. This cannot be attributed to changes in dose rates over burial time as these would have affected all dated fractions in the same direction. The age–depth plot (Fig. 4 right) visualizes that in the lower part (below L1LL2, samples BK1 to BK5) coarse-grain quartz ages systematically underestimate middle-grain quartz ages, which themselves underestimate the pIRIR$_{290}$ ages. These results argue for a longer-lasting hiatus within or at the base of the L1SS1 palaeosol (see above) and a very long hiatus within the S1 pedocomplex. The pIRIR$_{290}$ age of BK2

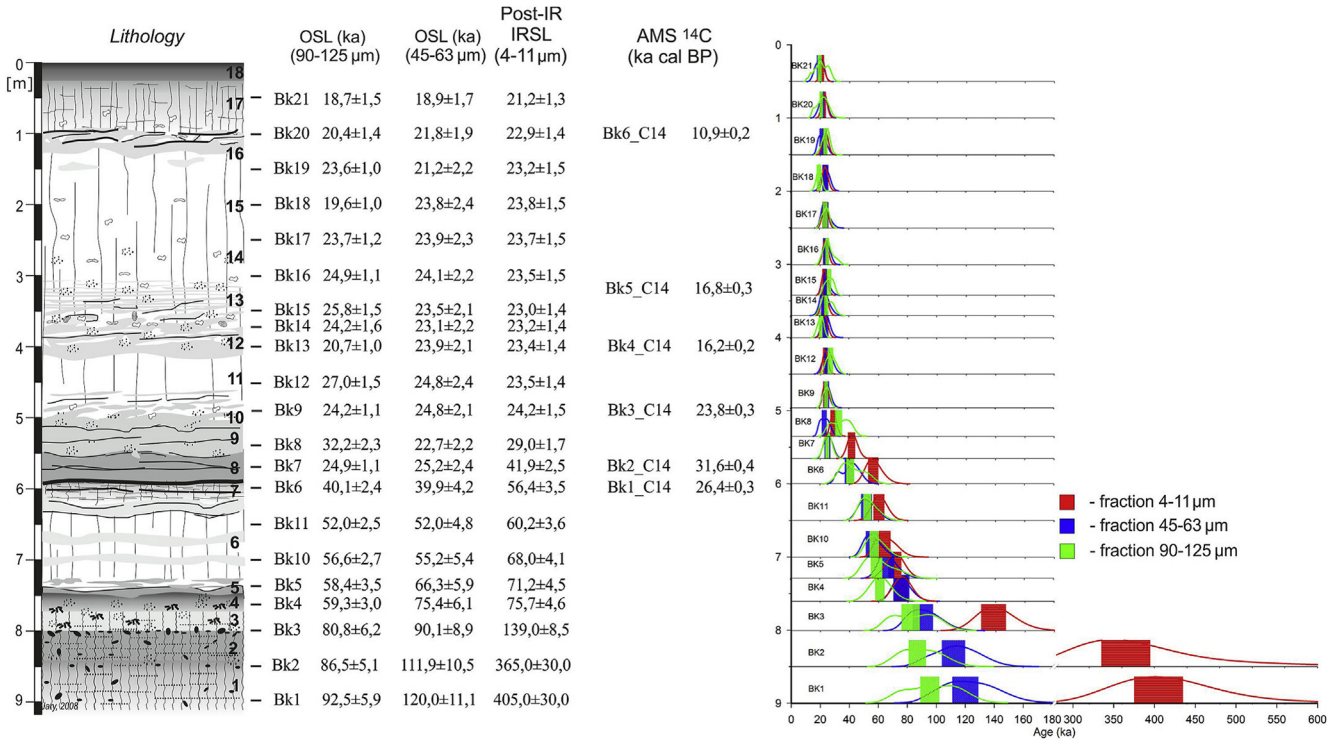

Figure 4. OSL ages from middle and coarse quartz grains and $pIRIR_{290}$ ages from fine polymineral grains obtained from the Biały Kościół (2009) section in the Gliwice laboratory (from Moska et al., 2019).

(365 ± 30 ka) agrees with the $pIRIR_{290}$ age of BT 1668 (343 ± 18 ka, with $a = 0.085$, which is similar to the value used for BK2). Despite some differences between the ages obtained in Gliwice and in Bayreuth, which will be discussed later, the comparison of the dataset from both laboratories evidences amazing accordance.

3.2 The surprise – Zaprężyn

The exposure near the village of Zaprężyn is situated at 51°14′43.7″ N, 17°11′51.8″ E at ca. 164 m a.s.l. in hilly ground at the southern end of the terminal moraine belt of the Wartanian stage (Saalian glaciation; Krzyszkowski, 1993). At the city of Trzebnica the terminal moraine (Winna Góra) is suggested to correlate to the Odranian stage (Jary and Krzyszkowski, 1994). It is supposed that the LPS rests on top of a Wartanian outwash cone; the hilly country in the surroundings may, however, also reflect a number of relatively small gredas (elongate loess ridge) (Różycki, 1967; Léger, 1990). Two horizons with ice wedge pseudomorphs were reported from the Zaprężyn section (Jary, 2009; Jary et al., 2011; Jary and Ciszek, 2013), but during sampling for OSL dating in September 2015, the lower one was no longer visible due to collapse and overgrowth of this part of the exposure. For sampling in 2015, we widened the excavation to the left where the upper ice wedge pseudomorphs' horizon was seen best (Fig. 5, at the spade). An erosional unconformity rising from the left to the right could then be followed over the whole length of the wall. It manifests itself as a tiny bed of fine sand some millimetres thick and will have an important role for the interpretation of the OSL ages. Loess and sandy loess above the unconformity are attributed to L1LL1 and loess below it to L1LL2 with a not yet clearly defined lower boundary with S1 supposed to lie between 5.3 and 6.0 m depth.

An exposed section of the ice wedge cast network and thermokarst features is shown in Fig. 6. At its top gelifluction tongues dipping slightly to the left are a result of permafrost decay. These elongated tongues are overlain by more or less parallel bedded sandy loess.

Based on previous ^{14}C AMS ages mentioned by Jary (2007, their Table 7, Poz-7998 and Poz-7649), the ice wedge pseudomorphs were supposed to originate from the LGM. This would fit well for the upper ice wedge pseudomorphs. Our within-error-bar stratigraphically consistent OSL quartz ages, however, contradict this opinion for the ice wedge pseudomorphs shown in Figs. 5 and 6. The OSL quartz ages are plotted in Fig. 7, together with the ^{14}C AMS ages. The OSL ages from Bayreuth suggest that the ice wedge formed earlier than 52.5 ± 3.7 ka (sample 12) and 56.8 ± 4.7 ka (sample 11) and later than 68.2 ± 5.6 ka (sample 10) and 64.7 ± 4.7 ka (sample 9), respectively. The oldest ^{14}C AMS age (> 50 ka BP, Poz-6939) from a humic layer OSL-dated to 95.7 ± 6.6 ka (sample 3) does not conflict with

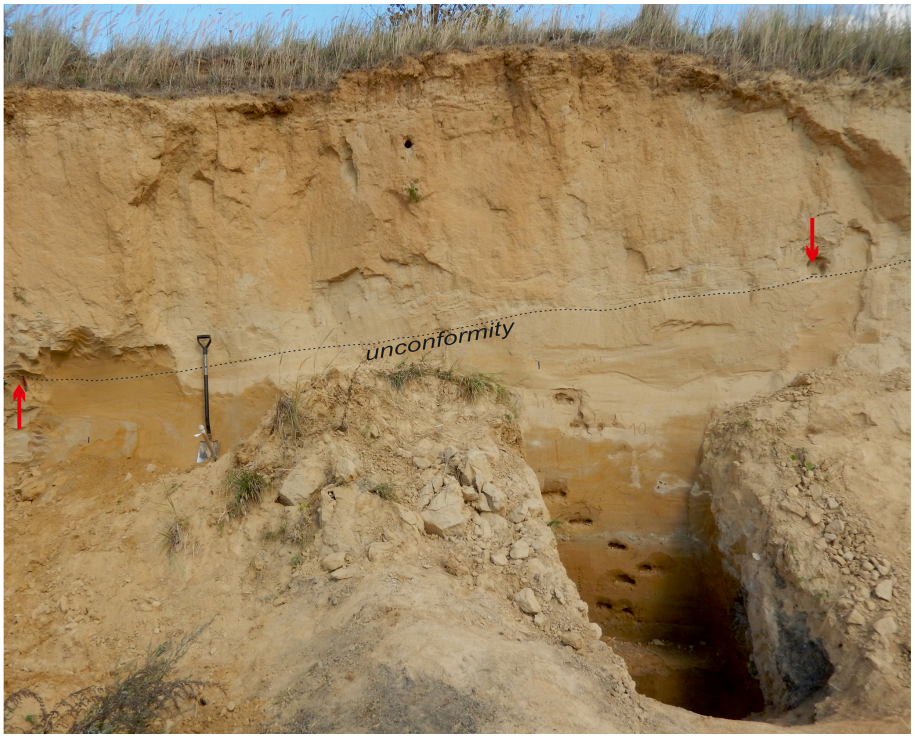

Figure 5. The Zaprężyn exploratory excavation in September 2015. The unconformity is visualized by the dotted line. Sample ZAPR12 (Bayreuth) was taken immediately below the unconformity at the left margin of the photo at the red pocket knife (red arrow upwards) and sample 13 immediately above the unconformity at the right (red arrow downwards). All other Bayreuth samples were extracted at the trench.

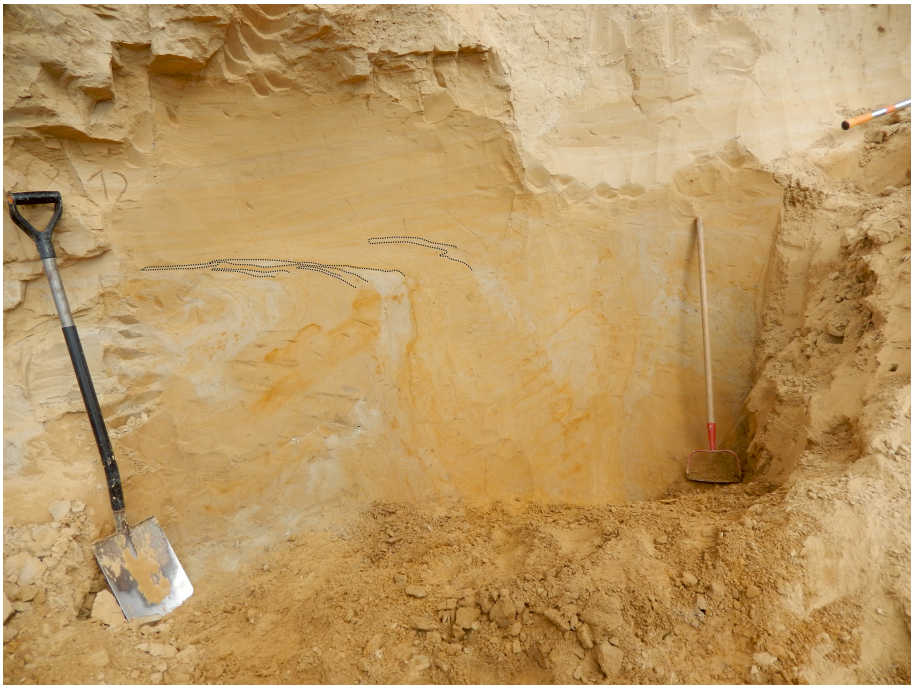

Figure 6. Detail of the Zaprężyn exposure in September 2015. Ice wedge pseudomorphs are visible to the left of the scraper (red tool) and its handle. Gelifluction tongues traced by greyish gleyed loess bend to the left and are overlain by striped brownish sandy loess. The position of OSL sample 12 is marked on top of the spade. Some of the gelifluction lobes are traced by dotted black lines.

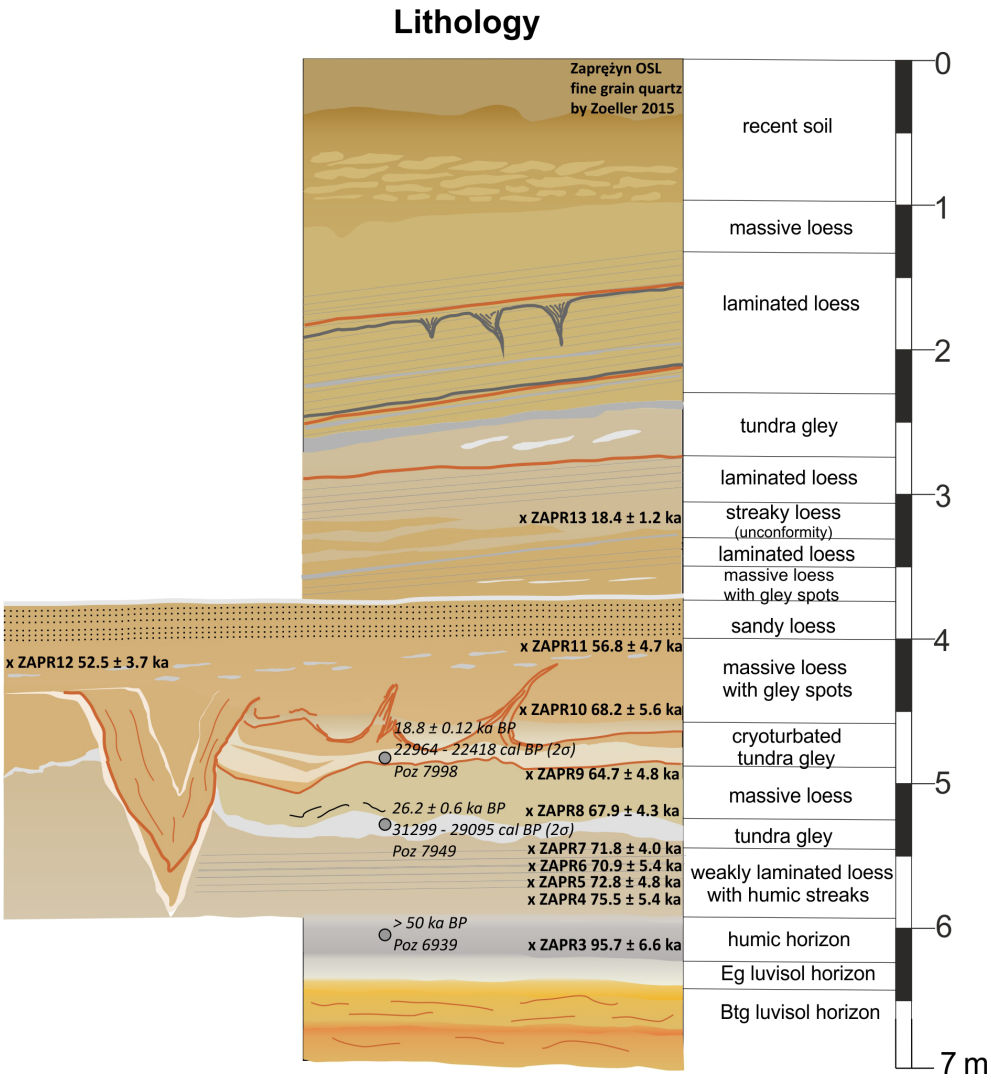

Figure 7. The Zaprężyn section with OSL ages (fine quartz grains) obtained in the Bayreuth laboratory and former ^{14}C AMS ages (Jary, 2007, grey circles).

the OSL ages. Despite some evidence for age underestimation also from quartz OSL ages, which will be discussed further below, the mentioned unconformity appears to represent a time span of ca. 29 to 39 ka in which the L1SS1 is to be expected but is denuded here. Formation of sandy loess above the unconformity starts at 18.4 ± 1.2 ka (sample 13), and gley horizons below the unconformity appear too old for L1SS1.

OSL ages from the 45–63 µm quartz fraction which were taken for the Gliwice laboratory will be published and discussed elsewhere. Marcin Krawczyk plotted the sampling positions (2015) for the Bayreuth laboratory in an informative design reflecting the soil colour, periglacial features and spatial distribution of the samples along the exposure (Fig. 7). Fine-grain quartz OSL ages obtained in Bayreuth are shown together with earlier published (Jary, 2007) ^{14}C AMS ages. In Fig. S1 the results are plotted in an older diagram which was used during sampling. Grain size composition of the profile is presented in Fig. S7.

3.3 The Sandomierz Upland key section – Złota

The sampled wall of the Złota section is situated at the southern margin of the Sandomierz Upland at 50°39′11″ N, 21°39′53″ E close to the Vistula. The exposed LPS including the entire last glacial–interglacial cycle is 13 m thick and reaches up to ca. 170 m a.s.l. The neighbouring but no-longer-accessible former loess exposure Polanów Samborzecki (Jary, 2007), which was studied for many years, is only some 200 m away. Previous research is outlined in Moska et al. (2015, 2018).

The L1SS1 pedocomplex is described to be up to 2 m thick and, thus, offers a good opportunity to study this interstadial soil complex and to contextualize it on the timescale.

As a detailed luminescence chronology of the whole section was already supplied by Moska et al. (2018, 2015) using middle quartz grains and fine polymineral grains, our sampling for the Bayreuth laboratory in September 2015 focused on the L1SS1 pedocomplex. Six samples were extracted between 6.0 and 7.75 m depth. The exploratory excavation from which the Gliwice samples were taken in 2012 had to be cleaned again and some decimetres of material removed. Thus, sample material for Gliwice and Bayreuth was not identical, but the Bayreuth samples could be unambiguously identified in the lithological profile of Moska et al. (2015).

Figure 8 shows on the right the whole profile at Złota, exhibiting the 25 pedo-sedimentary units distinguished during October 2013 fieldwork, with the zoomed-in part around L1SS1 with OSL ages of samples ZL-1 to ZL-6 from the Bayreuth laboratory on the left (field design by Pierre Antoine). The ages are stratigraphically consistent with mean ages of 26.5 to 27.6 ka (ZL-4, tundra gley, to ZL-6, all from L1LL1) above the L1SS1 palaeosol. The ages of ZL-3 (31.9 ± 1.9 ka, upper part of L1SS1, doubled tundra gley) and ZL-2 (38.6 ± 3.6 ka, lower part of L1SS1, brown soil) argue for a pedocomplex developed under different environmental conditions. Sample ZL-1 (50.0 ± 5.4 ka) originates from the unweathered loess L1LL2. If the L1SS1 pedocomplex is perceived as comprising units 13, 14, and 15a and unit 12 is taken out as a discrete palaeosol (tundra gley), the formation of L1SS1 at Złota can be narrowed down to between ca. 30 and ca. 40 ka.

Dating results obtained in the Gliwice laboratory are presented in Fig. 9 (from Moska et al., 2018, cut out from their Fig. 3). Note that the older lithostratigraphic nomenclature (L1L1, L1S1, L1L2) was used in this figure. For the L1LL1 and the top of L1SS1 (sample Złota9), loess quartz OSL ages (45–63 µm) and $pIRIR_{290}$ ages (fine polymineral grains) agree well, with the exception of the quartz age of sample Złota10 (inversion). For all stratigraphically older samples (Złota1 to Złota8), the quartz ages significantly underestimate the $pIRIR_{290}$ ages, which are stratigraphically consistent and correspond to geologically expected ages. It is worthwhile noting that even for the oldest samples from loess below S1 (142 ± 9 and 150 ± 12 ka, respectively), there is no indication of age underestimation. Comparing the Gliwice ages with those from Bayreuth (Fig. 8a), agreement of quartz ages is found despite the different grain sizes, with the exception of Złota10. As the quartz ages of samples Złota7 and Złota6 underestimate their $pIRIR_{290}$ ages, this must also be considered for the sample ZL-1 from Bayreuth (50.0 ± 5.4 ka). For the other quartz ages (4–11 µm) from Bayreuth, agreement with the $pIRIR_{290}$ ages is observed.

3.4 Ice wedges and thermokarst features in Upper Plenivistulian loess L1LL1 – Tyszowce

The village of Tyszowce is situated ca. 110 km southeast of the city of Lublin in the very east of Poland (Volhynian Upland) close to the Ukrainian border. The profile with exposed loess cover of 19 m (14 m thick L1LL1 above L1SS1!) was studied by Moska et al. (2017); samples for luminescence dating in Gliwice were taken in 2012 a few metres to the right of our trench visible in Figs. 10a and 11a.

This section was, however, no longer fully accessible, and for our own sampling in September 2015, a new 16 m deep trench had to be created by a shovel excavator followed by cleaning by hand. The coordinates were measured by GPS, yielding 50°36′29.1″ N, 23°42′38.6″ E and the top of the section at ca. 220 m a.s.l. In this new trench the L1SS1 was – in contrast to the former profile – more or less eroded as a result of periglacial dynamics (Fig. 10) and only some geliflucted or cryoturbated lumps evidenced the former existence of the pedocomplex (Fig. 10b). Thus, the ages published by Moska et al. (2017) cannot always smoothly be transferred to the new profile. Our sampling focused on the supposed remnants of L1SS1 and the onset of L1LL1.

OSL samples TYS 1 to TYS 4 (Figs. 10a and 11a) are closely spaced at intervals of 20 to 35 cm at depths of 11.0 m (TYS 1), 11.2 m (TYS 2), 11.45 m (TYS 3), and 11.8 m (TYS 4) on the right-hand side of the ice wedge pseudomorph which begins between TYS 3 and TYS 4. Samples TYS 5 to TYS 7 were extracted to the left of the ice wedge pseudomorph at 14 m (TYS 5) and ca. 16 m depth (TYS 6 and TYS 7, Fig. 11b). The position of all OSL samples in the entire profile is shown in Fig. 11a, with OSL ages of the fine-grain quartz fraction.

The ice wedge pseudomorph begins between samples TYS 4 (pre-dating the ice wedging) and TYS 3 (post-dating it as well as TYS 2 and TYS 1, horizontal bedding; Figs. 10a and 12). The ice wedging can thus be bracketed anywhere between ca. 30 and 25 ka, younger than L1SS1, which at Tyszowce is dated at around 40 ± 3 ka (Moska et al., 2017). The OSL age of TYS 7 (43.3 ± 3.0 ka, gley lump in a deeper position of the thermokarst, Fig. 11b) is identical within uncertainties and argues for affiliation of this gley remnant to L1SS1. The OSL age of TYS 6 (brown clayey loess, 67.9 ± 7.0 ka), however, attributes this material rather to L1LL2 or even to S1 (cf. Moska et al., 2017). The stratigraphic and geological storage conditions of this lump or bed appearing like a foreign body could, unfortunately, not be dug up further.

Comparing ages given by Moska et al. (2017) with our own ages (Fig. 11b) is not always straightforward because we did not use identical sample material and, in particular, due to the strong periglacial destruction observed in the 2015 excavation. For the entire set of luminescence ages from the Gliwice laboratory for the Tyszowce section, see Fig. 12, in which L1LL2 is only ca. 1.5 m thick (15.5 to 17 m depth) above S1. Some pIRIR ages from the Gliwice laboratory are projected onto the 2015 profile. For the horizontally bedded layers above the ice wedge cast (TYS 1, TYS 2, TYS 3), a comparison should be justified and the fine-grain quartz ages turn out to be older than the middle-grain quartz ages

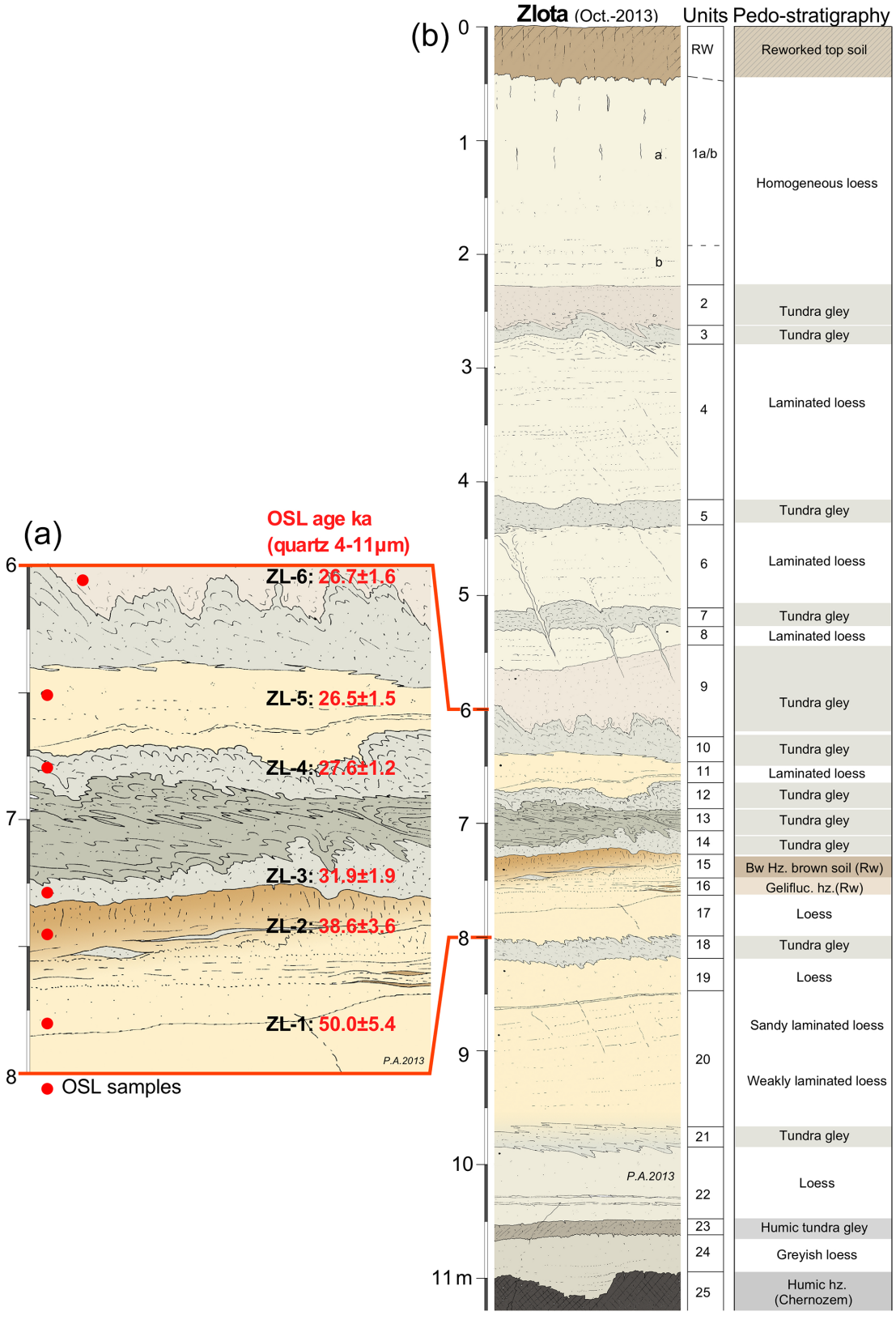

Figure 8. The profile at Złota (October 2013) **(b)** and the zoomed-in part around L1SS1 with OSL ages of samples ZL-1 to ZL-6 from the Bayreuth laboratory **(a)** (Pierre Antoine).

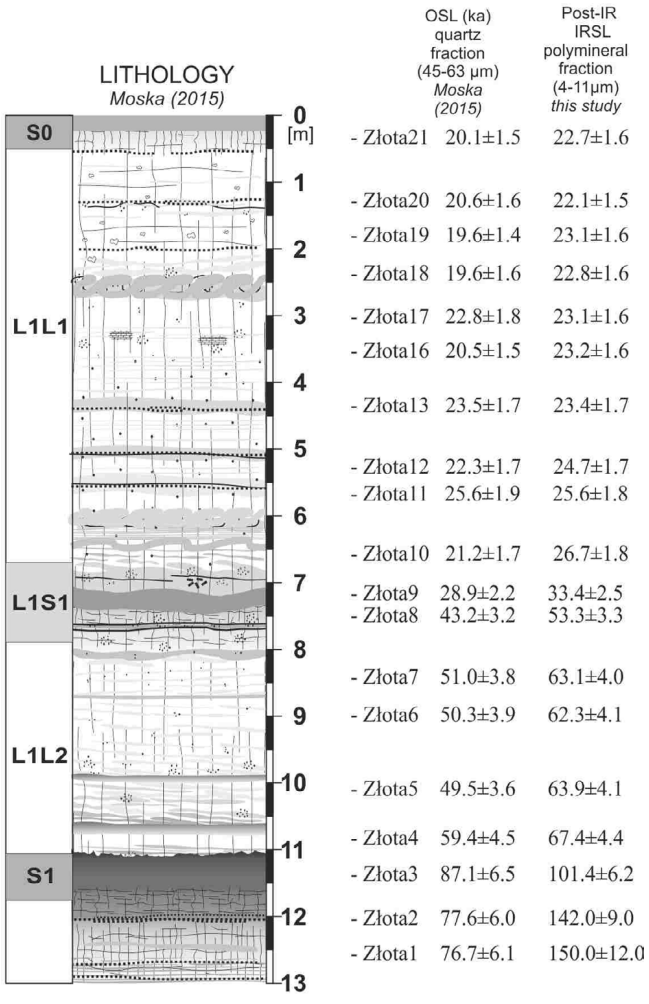

Figure 9. Luminescence ages from the Złota section obtained in the Gliwice laboratory (from Moska et al., 2018, cut out of Fig. 3).

(TYSZ_11, TYSZ_10; see also TYSZ_9 and TYSZ_8 in Fig. 12). The pIRIR ages of Moska et al. (2017) in the section shown in Fig. 11b, however, confirm their quartz ages with the exception of TYSZ_5 (55.5 ± 3.2 ka).

4 Discussion

The results presented above will be discussed from two aspects: (i) results for the individual profiles and (ii) general discussion focusing on the implications of different luminescence dating protocols.

4.1 Individual profiles

The fine-grain quartz ages from the Biały Kościół profile (2018, Fig. 3) are in stratigraphic order within uncertainties and do not conflict with the age conceptions of Jary and Ciszek (2013), with the exception of the oldest sample BT 1688, the quartz age of which is regarded as underestimated with respect to its deposition prior to S1 pedogenesis. It appears strange however that samples BT 1671 to BT 1674 from the L1LL2 loess yield a mean age value of 58.7 ka without any noticeable increase with depth. These samples under debate have equivalent doses of around 200 Gy (Table S1), which are considerably beyond the threshold value of ca. 100 Gy suggested for reliable OSL dating by Timar-Gabor et al. (2017) without rigorously ruling out higher doses as suggested by Avram et al. (2020), who estimate ∼ 150 to ∼ 250 Gy as a threshold value. Complete trust in these ages would imply that this up to 2 m thick loess including some weak tundra gleys was deposited very rapidly at the transition from MIS 4 to MIS 3. This is not impossible but sounds challenging. Therefore some age underestimation of these quartz ages must be taken into account (see also general discussion below). This assumption is supported by the pIRIR ages, which, however, may be somewhat overestimated due to a residual dose at deposition (in particular sample 1672, which may be derived from a bed mixed up with geliflucted material; see the bulge of the age–depth plot in Fig. 3 above BT 1671 for both pIRIR and OSL ages). In the Bayreuth laboratory it was not attempted to find a residual dose beyond the background subtraction as explained above. There is no proof at all that a subtraction of an experimentally approximated residual background dose would meet a natural residual at deposition better (cf. Avram et al., 2020). The close parallel courses of the age–depth plots (Fig. 3) between samples BT 1679 and BT 1677 can in fact be interpreted as an offset due to uncorrected residual doses of the pIRIR ages. Apart from BT 1672 the pIRIR ages are in agreement with the attribution of L1LL2 to MIS 4. A similar behaviour of fine-grain quartz and polymineral ages is seen in the data given by Moska et al. (2019). Their pIRIR ages in particular also argue for a MIS 4 age of the L1LL2, whereas quartz ages from this loess are also ambiguous and are prone to underestimation.

With respect to the stimulating publication by Lüthgens et al. (2020), another solution imposes on the discussion. The local LGM of the Ristinge (and probably Ellund–Warnow) ice advance (50 to 55 kyr old) affected mainly the southwestern part of the Baltic Sea and adjacent areas, most probably surrounded by a belt of harsh periglacial conditions. If the fine-grain quartz ages around 55 to 60 ka (±5 % to 7 %) are correct, the L1LL2 or at least its upper part including periglacial features may be attributed to this ice advance mirroring its periglacial surroundings. This interpretation would imply age overestimates of corresponding pIRIR ages.

Quartz ages (middle and coarse grains) from the L1LL1 obtained in Gliwice tend to be lower than those obtained in Bayreuth (fine grains), but this cannot be confirmed for the stratigraphically older samples. Our findings in the Gliwice and Bayreuth laboratories appear opposed to those of Avram et al. (2020) and Timar-Gabor et al. (2017) and may complicate the problem further. But a general rule relating to a grain size dependence of quartz ages cannot be supported

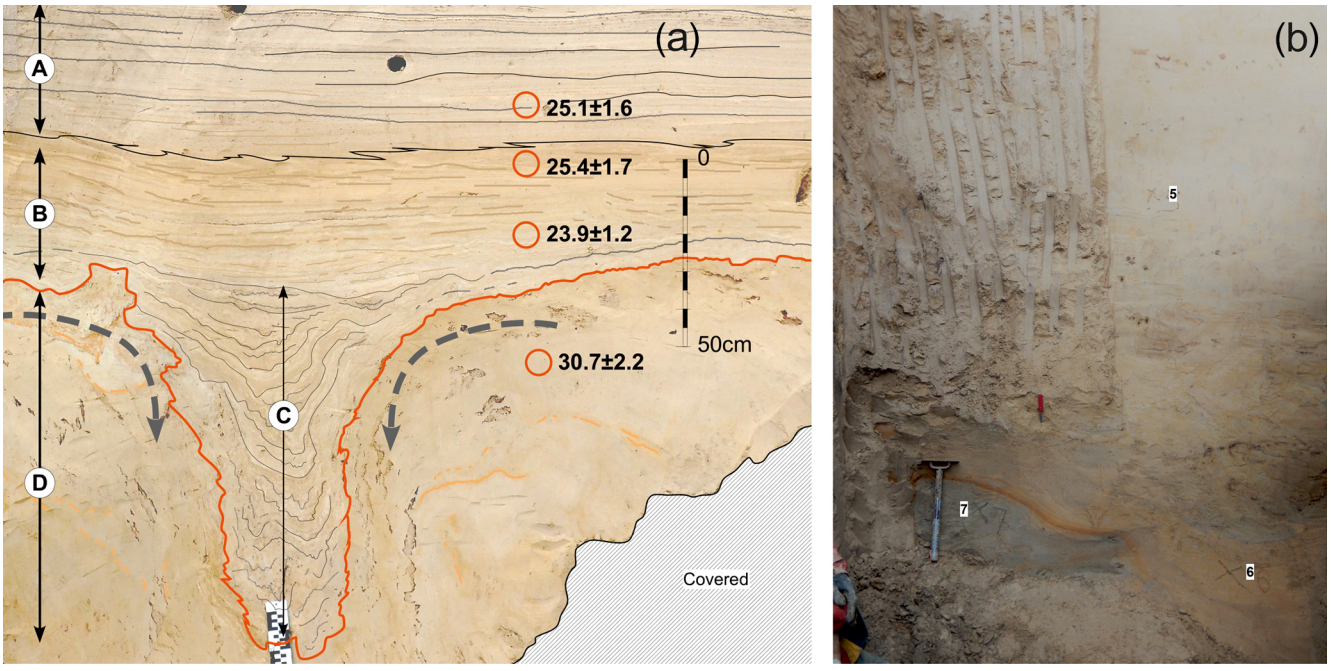

Figure 10. Tyszowce section. **(a)** Ice wedge pseudomorph (lower left corner) and brownish and greyish cryoturbated remnants of an interstadial soil. Explanatory drawing of the situation after a photo (Pierre Antoine). OSL ages (ka) of samples 1 to 4. A: very finely laminated (≤ 5 mm thick) light yellowish grey calcareous loess with sub-continuous undulated black lines of manganese oxide (cryptogamic crust remnants?). B: laminated calcareous loess with light brown to orange oxidation bands and hillwash stratifications (partly translocated by hillwash processes/small cross laminations). C: irregular hydromorphic loessic infilling of a former large ice wedge pseudomorph (> 100 cm $\times$ 60 cm) resulting from the collapse by gelifluction of the permafrost active layer (hydromorphic loess/greyish patches). D: homogeneous and dense pale yellowish calcareous loess with some orange oxidation lines and abundant black manganese oxide patches and lines (upper horizon of a former permafrost). **(b)** Thermokarst gelifluction lobe (grey, sample 7 lower left) from a clayey palaeosol (tundra gley, L1SS1?) beside the ice wedge pseudomorph, kneaded with older brownish and clayey loess (sample 6). Sample 5 (upper right) is from greyish brown reworked loess with streaks of a tundra gley, less compacted than samples 6 and 7.

by the data from the Biały Kościół section. It is supposable that such dependence exists but is concealed by different source areas of the lithological units. For Biały Kościół two major source areas must be considered: the northern glaciogenic area such as the Odra Pradolina (glacial valley, "Great Odra Valley"; Badura et al., 2013; Waroszewski et al., 2021) and the southern mountainous area dominated by Palaeozoic rocks of the Sudetes Mountains. In a periglacial environment with frequently changing wind directions, a frequent change of these main source areas is conceivably delivering quartz grains of different geological histories and different luminescence characteristics. The aeolian transport distance of different grain sizes superimposes this effect. So far, however, it can only be speculated about whether the unsteady behaviour of quartz luminescence at Biały Kościół can be explained. As a consequence, some geochronological questions at the Biały Kościół section such as the exact timing of the L1SS1 at this site can hardly be decided based on the quartz ages alone.

The $pIRIR_{290}$ ages from both luminescence laboratories are more consistent, but they are prone to age overestimates due to incomplete bleaching, independent of the question of whether a residual dose estimated by laboratory experiments is subtracted or not. In the case of the Biały Kościół section this subtraction as executed by Moska et al. (2019) appears to be justified. Nevertheless, the exact time bracketing of the L1SS1 remains challenging. If it is accepted that the quartz ages within and below L1SS1 are underestimated but the $pIRIR_{290}$ ages are perhaps overestimated, the true ages should lie in between. The evidence for a hiatus lasting many thousands of years within the L1SS1 suggests that at Biały Kościół the L1SS1 is not a pedocomplex but a complex (of soil remnants separated by erosion events and sediments) and, thus, a parallel to the Gleina Complex (Meszner et al., 2013) in Saxonian loess, eastern Germany. Consequently, the L1SS1 at the Biały Kościół section may not represent its complete and typical development as described elsewhere, for example, at Złota (see below). The unexpectedly high pIRIR ages (> 300 ka) of the lowermost samples (BT 1668 and Bk 2 and 1) may be affected by the $pIRIR_{290}$ dose overestimation recently described by Avram et al. (2020) and should be interpreted very cautiously, as they found that beyond ca. 400 Gy the natural $pIRIR_{290}$ signals overestimate the laboratory signals, implying age overestimates.

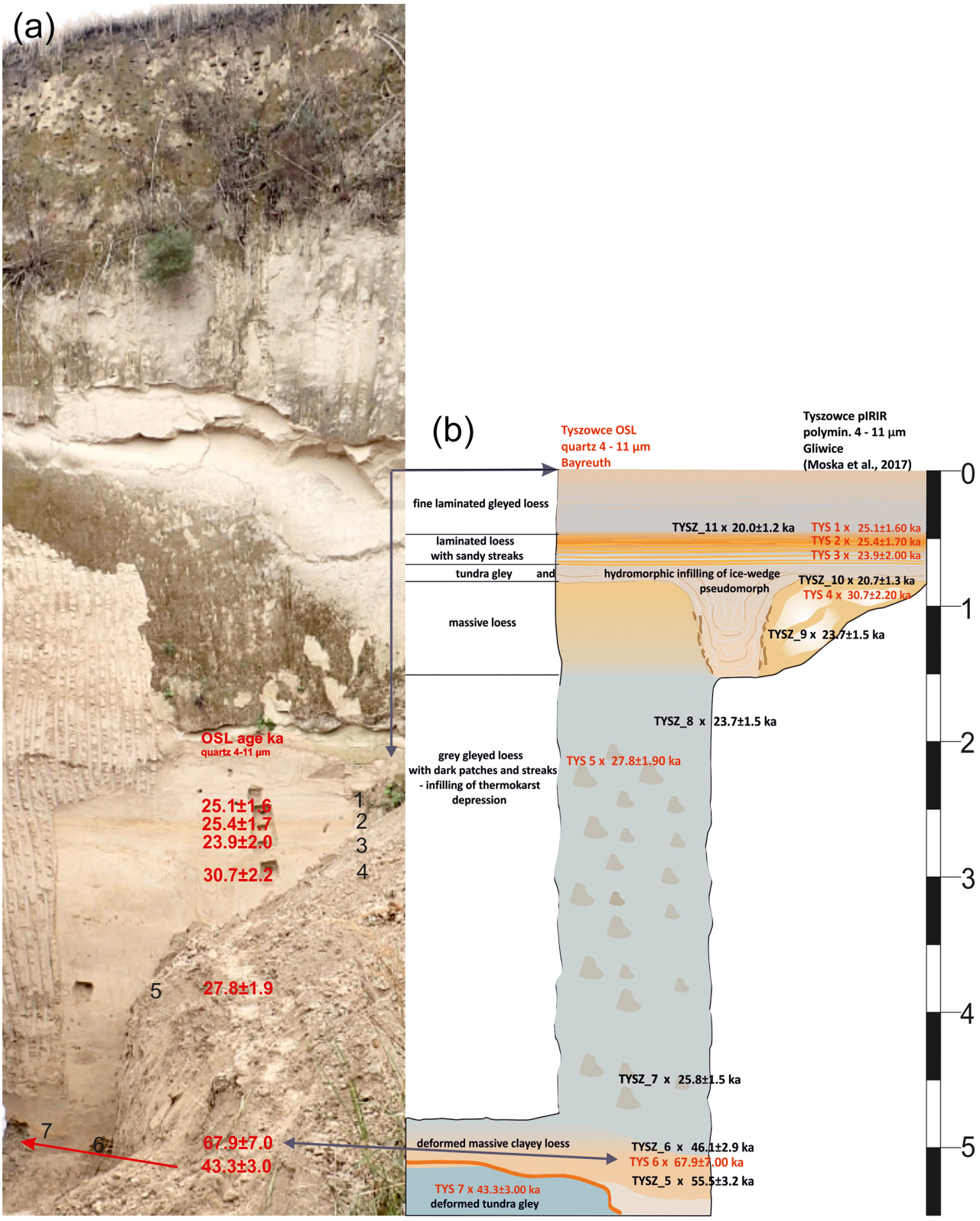

Figure 11. **(a)** The Tyszowce trench (16 m) from September 2015 with all OSL samples for the Bayreuth laboratory and their OSL ages (red). **(b)** Attempt to compile quartz OSL and polymineral pIRIR ages for the two trenches (2012 and 2015) of the Tyszowce section in a schematic plot (Marcin Krawczyk). Red characters: fine-grain quartz ages obtained in the Bayreuth laboratory. Black characters: selection of fine-grain polymineral pIRIR ages obtained in the Gliwice laboratory (from Moska et al., 2017) which are relevant for comparison with ages from the Bayreuth laboratory. Please note the different notation of Bayreuth samples (e.g. TYS 6) and Gliwice samples (TYSZ_6).

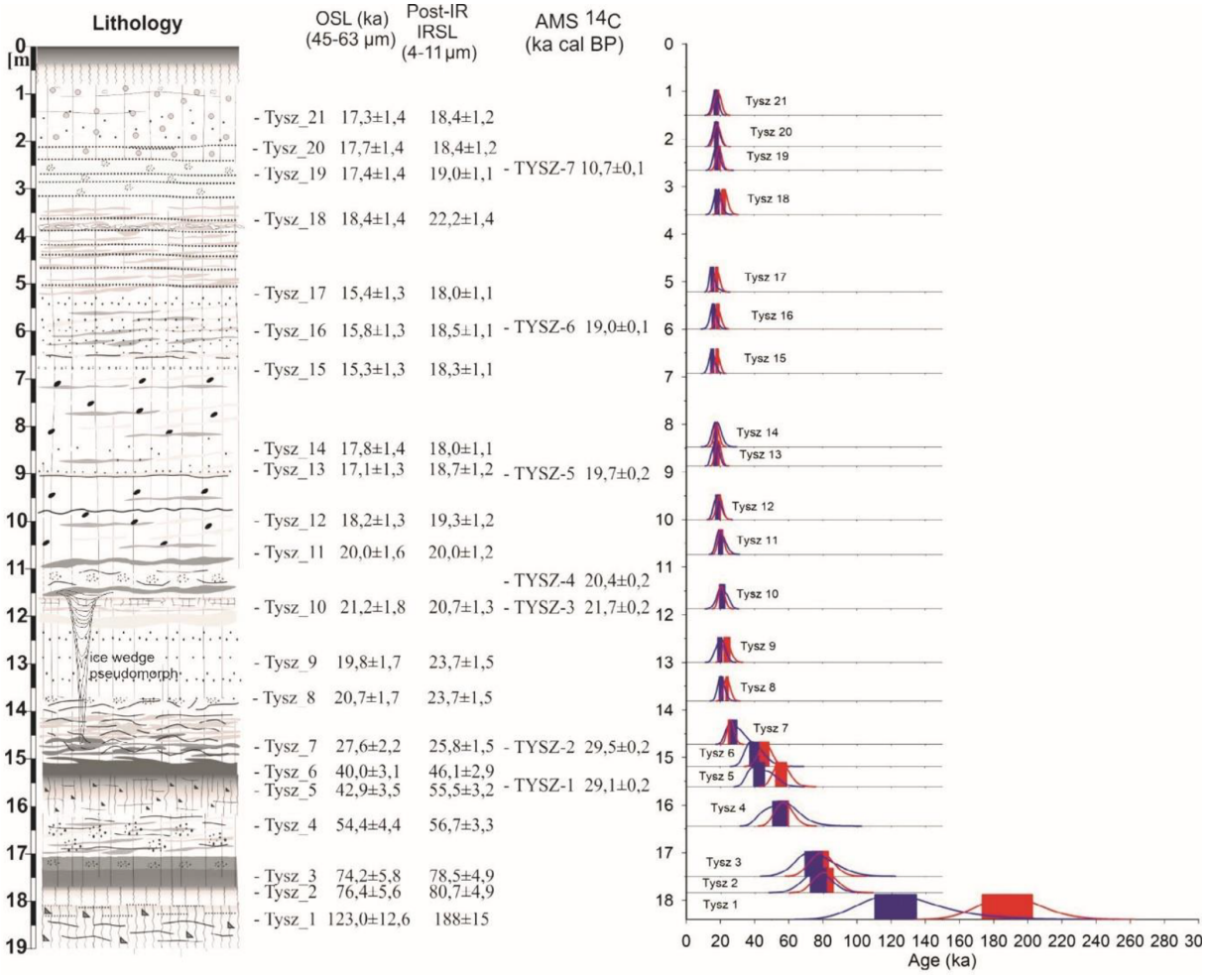

Figure 12. Lithology, OSL and pIRIR ages, radiocarbon ages, and relative probability plots for ages obtained for all samples versus depth at Tyszowce according to Moska et al. (2017). The ice wedge pseudomorph position is now marked.

At the Zaprężyn section the fine-grain quartz OSL ages from the Bayreuth laboratory (Figs. 7 and S1) indicate that the L1SS1 is completely missing. According to the fine-grain quartz ages (ZAPR8, ZAPR9, and ZAPR10), the loess deposited prior to the ice wedging can be attributed to MIS 4 and the age of ZAPR11 (sandy loess, 56.8 ± 4.7 ka) cannot clearly be allocated to MIS 4 or MIS 3, whereas ZAPR12 (lamellar sandy loess, 52.5 ± 3.7 ka) deposited after the melt out of the thermokarst argues for MIS 3. The lithology of the flashy loess with sand lamellas, however, supports cold windy climate conditions rather than a more temperate interstadial. Thus, this sandy loess (samples ZAPR11 and ZAPR12) may also mirror periglacial conditions caused by the Ristinge ice advance (see above).

From the profiles investigated in this study, Złota is best suited to bracketing the duration of soil formation of the L1SS1 pedocomplex between ca. 30 and 40 ka (see above). It comprises a lower brown (cambic) soil and an upper tundra gley soil with signs of gelifluction and cryoturbation. The L1SS1 at the Złota section is comparable to but not identical with the "Lohne Soil" in southern Germany (cf. Rousseau et al., 2017; Moine et al., 2017). Before or during the formation of the tundra gley, deposition of fresh loess started, as evidenced by the OSL age of ZL-3 (31.9 ± 1.9 ka) being significantly younger than ZL-2 (38.6 ± 3.6 ka) from the brown loess. ZL-3 gives evidence for the presence of ca. 32 kyr old loess, which had not been identified so far in the previous sections from Silesia. The age of the first great loess accumulation phase of what is called the Upper Pleniglacial in northern France, Belgium, and western Germany is also 31–32 ka (Antoine et al., 2015). OSL characteristics of fine-grained quartz confirm the change of parent material between ZL-2 and ZL-3: ZL-1 and ZL-2 are characterized by unusually low OSL sensitivity, in contrast to ZL-3 and samples positioned farther upwards. The tundra gley on top of L1SS1 (ZL-4, 27.6 ± 2.0 ka, unit 12) is regarded as a separate soil not included in L1SS1 but belonging to L1LL1. We attribute the relative complete stratigraphy of this part of the profile to

both the more continental climate referred to Silesia and to the proximity of the main source of the loess (Vistula valley). No inversions of fine-grain quartz ages were observed.

The reliability of the fine-grain quartz age of ZL-1 (50.0 ± 5.4 ka) from the L1LL2 loess (unit 17), however, can hardly be judged due to the lack of further fine-grain quartz samples from the L1LL2. Złota lies some 330 km south-southeast of Zaprężyn, and it appears very questionable whether the periglacial impact of the regional Ristinge ice advance could reach up to Złota. The consistent pIRIR ages by Moska et al. (2018) from the L1LL2 loess at Złota (ca. 62 to 67 ka) argue for attribution to MIS 4 and for a severe age underestimate of all the quartz ages from L1LL2. The obvious presence of ca. 32 ka loess (ZL-3) may, however, be connected with the extended Odra ice lobe of the Klintholm ice advance 30–34 kyr ago (Lüthgens et al., 2020; Figs. 4 and 5). Despite its potentially speculative character, this possibility deserves further discussion and attention, thereby considering that the ice-induced trigger of the climatic deterioration 30–34 kyr ago was superimposed by Heinrich Event 3 (H3), clearly reflected in LPSs of western central Europe (Antoine et al., 2015; Moine et al., 2017) and southwestern Europe (Wolf et al., 2018).

At the Tyszowce section two questions deserve discussion: the timing of the ice wedging and of the thermokarst processes and the age differences between the Gliwice and the Bayreuth laboratories for samples from L1LL1. As mentioned above, the two laboratories could not execute their dating using identical sample material. Moska et al. (2017) did not mention the ice wedge pseudomorph and the thermokarst, but strong periglacial reworking is evident from their Fig. 4 above L1SS1 between ca. 13.5 and ca. 15 m depth, connected with a considerable jump in luminescence ages (middle quartz grains and fine pIRIR grains). In Fig. 12 all luminescence ages obtained in Gliwice are plotted together with some AMS ^{14}C ages and the position of the ice wedge pseudomorph. The timing of the ice wedging cannot be directly derived from their ages but indirectly between ca. 29.5 ka cal BP (AMS ^{14}C, GdA-3133 TYSZ_1) and ca. 20 ka (TYSZ_11 and TYSZ_4). According to the OSL ages from Bayreuth, the ice wedging and subsequent thermokarst is bracketed between ca. 30 and ca. 25 ka, at the beginning of MIS 2 but posterior to the Klintholm ice advance. It is interesting to note that ice wedging in loess of northern France also occurred in the same time span at about 27–28 ka (levels F2–F3), whereas the main level F4 at ±32–31 ka (Antoine et al., 2014) was in time with the Klintholm advance. The ice wedging at Tyszowce, however, apparently pre-dates the Pomeranian ice advance triggered by a slight interstadial warming (Lüthgens et al., 2020) and rather witnesses a very cold and continental climate phase starving a major ice advance. Because of the limited depth and width of the 2015 dredge hole, it cannot clearly be decided if the thermokarst features in the lowermost part of the dredge hole are genetically related to this ice wedging or if they are older (MIS 3 or MIS 4; see Zaprężyn above).

The Bayreuth sample TYS 1 and the Gliwice sample TYSZ_11 originate from the same loess bed (for sample positions see Figs. 11b and 10a, unit "A"). Although non-identical sample material was dated, these two quartz OSL ages are particularly suitable for direct comparison. For sample TYSZ_11 (19.1 ± 1.4 ka for quartz 45–63 µm, differently from Fig. 4 in Moska et al., 2017, reproduced here as Fig. 12), exemplarily the age is calculated by the ADELE program using dosimetric and D_e values given in Moska et al. (2017, their Table 2) and yields 19.9 ± 1.0 ka. The ratio of effective dose rates $\dot{D}_{\mathrm{Moska}}/\dot{D}_{\mathrm{Adele}}$ for sample TYSZ_11 is 1.04 (2.73 and 2.62 Gy ka^{-1}). This demonstrates that the dose rates calculated by different age calculation programs cannot account for the observed discrepancy of ages. If from the mean D_e obtained from fine quartz grains in Bayreuth (76.8 Gy) the $\dot{D}\alpha$ (0.374 mGy a^{-1}) acquired over 25 kyr (9.35 Gy) is subtracted, 67.45 Gy remains as an approach for the D_e of the 45–63 µm quartz fraction. Moska et al. (2017, Table 2) find only 52.2 Gy, however. This crystallizes that determination of D_e for different grain sizes of quartz is the reason for the age discrepancies rather than dosimetry. How far laboratory illumination, being more critical for the fast OSL component from quartz than for IRSL from feldspars, may have influenced the D_e values for quartz grains cannot be currently assessed but should be a matter of further discussions. Different procedures for calibration of radioactive sources should also be borne in mind.

4.2 General discussion

The preceding exemplary discussion of samples TYS 1 and TYSZ_11 leads to a more general problem regarding grain size dependence of quartz OSL ages. The question has been addressed for several years (e.g. Lowick and Preusser, 2011; Chapot et al., 2012; Kreutzer et al., 2012; Timar-Gabor and Wintle, 2013; Timar-Gabor et al., 2015, 2017; Moska et al., 2015, 2019; Avram et al., 2020; Schmidt et al., 2021). A general rule cannot be proposed so far, however, because observed grain size dependencies of quartz ages point in opposite directions. In contrast to the results from Polish loess as well as from Saxonian loess (Kreutzer et al., 2012), observations from Romanian loess, for example, yield lower ages for fine quartz grains than for coarse quartz grains. It is furthermore astonishing that mean quartz OSL ages mentioned in this paper often "jump" in the stratigraphic order or even show age inversions, whereas quoted mean pIRIR ages by Moska et al. (2017, 2018, 2019) from identical samples stay "well-behaved" in stratigraphic order. It can, however, also be seen from the above-discussed sections that some samples whose pIRIR ages appear overestimated with respect to neighbouring samples also show a higher (mean) quartz age referred to underlying samples (cf. BT 1672 and BT 1678 from Biały Kościół). This probably indicates in-

complete bleaching due to periglacial reworking, and such samples are in general impeded for exact luminescence dating independent from the dated mineral fraction and should be thoroughly checked sedimentologically and geomorphologically.

Since the overall successful adaption of the quartz OSL-SAR protocol to dating of loess from the last glacial cycle, it has been favoured over IRSL or pIRSL because of higher sensitivity to daylight and the absence of anomalous fading. The results presented and discussed here, however, cast some doubts on the reliability of the quartz OSL ages unless the mentioned problems are better understood and apparent age underestimates due to reasons other than anomalous fading can be ruled out. Uncorrected OSL sensitivity change and different growth curve shapes for natural and laboratory-regenerated signal growth with doses are debated (e.g. Schmidt et al., 2021). Even if the present database is not yet sufficient, it is very likely that the quartz problems arise from the origin and geological history of quartz grains and mainly affect loess samples older than L1SS1. With respect to feldspars, quartz appears to be a relatively simple mineral, but the crystallization of quartz grains is very variable between magmatic, metamorphic, diagenetic or hydrothermal origin. Furthermore, (optical) zeroing and dosing cycles differentiate the luminescence characteristics of quartz. Due to the high chemical and mechanical resistance of quartz, the grains are often frequently recycled and eventually carry a history of several hundred million years around with them. As far as distinct source areas of quartz grains in certain sediment can be identified, quite similar OSL characteristics may be expected, but aeolian sediments such as loess often consist of quartz grains from very different source areas due to frequent changes in wind directions and due to various transport distances (and transport processes such as fluvial-induced mixing). The latter are reflected in the mean grain size, and coarser-grained quartz may originate from other more local sources than far-travelled fine quartz grains. It is hypothesized that these considerations are, besides diverging natural and laboratory growth curves, a further key to understanding the above-discussed problems with quartz OSL ages, in particular the grain size dependence owing to various source areas in a geologically manifold landscape with parent rocks from the Precambrian to the Neozoic in the source areas, as is the case for Polish loess areas.

The $pIRIR_{290}$ lends itself as an alternative but implies a higher risk for age overestimation due to incomplete bleaching compared to OSL from quartz. Given the fact that no $pIRIR_{290}$ age underestimates have been evidenced from the Polish loess sections discussed above, the problem of anomalous fading has apparently been erased. In view of the pending question of whether a dose residual should be subtracted from the D_e values and, if so, how to reliably estimate the residual dose, $pIRIR_{290}$ ages are prone to overestimation.

What should be done? "As you like it" is not passable. From this point of view we can suggest utilizing a two- or threefold strategy including $pIRIR_{290}$ and quartz OSL ages, reasoning that the true age lies anywhere between. As a priori it is unknown in which direction a possible grain size dependence of quartz points, fine-grain quartz fractions and middle- or coarse-grain quartz fractions should be dated and the higher quartz age compared to the $pIRIR_{290}$ age. Even if this approach requires considerably more human resources and machine time and the "bracketed true age range" may often not be precise enough to decide the geoscientific question involved (e.g. MIS 4 or MIS 3), it recommends itself as the most honest way to interact with users from geosciences. A well-dated marker horizon, ideally a volcanic tephra layer such as the Campanian Ignimbrite tephra, would be most helpful in this context but unfortunately is not known from the sections studied here, other than in Romania (Fitzsimmons and Hambach, 2013; Scheidt et al., 2021).

Such missing reliable age control in particular for loess > 30 ka also hampers the discussion about loess equivalents of the Ristinge and the Klintholm ice advances, which can so far only be assumed based on the fine-grain quartz ages. With respect to the $pIRIR_{290}$ ages, fine-grain quartz ages from L1LL2 ≥ 50 ka also appear to be underestimated in some profiles, whereas in other ones there is no proof. Underestimation of representative past water content cannot account for the observed amount of quartz age underestimates with $D_e > \sim 150$ Gy if referred to $pIRIR_{290}$ ages. The debate remains open at this stage and, thus, a too close backing of MISs to loess chronostratigraphy not taking into account other steering mechanisms in continental areas may be premature.

Despite the discussed pending problems, we can state that for the first time basic agreement was found in an inter-laboratory luminescence dating comparison of loess in Poland. The Bayreuth and Gliwice laboratories have worked completely independently with Zdzisław Jary acting as the only link. The achieved progress with regard to previous attempts is respectable. The advantage of independent dating work implied, however, the unavoidable disadvantage of not working with identical sample material. This gap is going to be closed, as Piotr Moska kindly supplied remains of his samples from Złota (< 45 µm) to the Bayreuth laboratory. These samples are in progress in Bayreuth, and the results will be published together elsewhere.

5 Conclusions

In the Bayreuth Luminescence Laboratory (Germany), self-consistent chronologies for four loess palaeosol sequences (LPSs) were achieved using OSL dating of fine-grained quartz (4–11 µm). From one section (Biały Kościół) fine-grain $pIRIR_{290}$ dating yielded significantly higher ages for samples older than ca. 30 ka. In comparison with quartz (middle and coarse grains) OSL ages and fine-grain $pIRIR_{290}$ ages obtained in the Gliwice laboratory (Poland), agree-

ment to a large extent was found, unlike in previous interlaboratory comparison of Polish luminescence laboratories. A meaningful agreement is the bracketing down of the L1SS1 pedocomplex, a most important stratigraphic level in Visutlian LPSs, to ca. 30 to 40 ka. Nevertheless some age differences between the Bayreuth and the Gliwice data call for further discussion.

An indication of grain size dependence from quartz ages is observed but in a reverse direction to those reported from, for example, loess in Romania (Avram et al., 2020, with further references therein), and, with respect to our observations, no general rule concerning the quartz grain diameter and OSL age underestimate can be established. For our samples, quartz OSL ages of fine grains are higher than (or at least equal to) those of middle and/or coarse grains. Age underestimation may, however, also affect fine quartz grains still far away from dose saturation (e.g. Złota, ZL-1), and assuming permanent water saturation (25 ± 5 % instead of 15 ± 5 %) for this sample would increase the age by 10 % only (55.0 ± 5.9 ka; see discussion above in Sect. 2 on luminescence dating). Since such a general rule for grain size dependence of quartz OSL ages cannot be derived from the data discussed in this contribution, we suggest that the strange behaviour of quartz ages from different grain sizes is rather caused by various sources (ranging from Paleozoic crystalline rocks to Quaternary glacial drift) with very different geological and thermal histories and, consequently, different OSL characteristics of quartz grains. Local and remote sources contribute to varying extents to individual sedimentary beds of LPSs, thereby being sorted by very variable transport mechanisms (wind strength and wind direction). Thus, fine grains and coarser grains from an individual sample may be derived from diverse sources.

From $pIRIR_{290}$ ages mentioned here, we found, however, no indication of age underestimates but some probability of overestimates caused by residual doses which cannot be estimated accurately, in particular for samples reworked under periglacial conditions. Determining $pIRIR_{290}$ ages complementing quartz ages is therefore advised for verification of quartz ages.

In the Zaprężyn section (Lower Silesia) ice wedging and subsequent thermokarst erosion more than 50 kyr old can be proved in loess below a long-lasting but hardly visible discordance, which completely removed the L1SS1 pedocomplex. In combination with the Tyszowce section (Volyn Hills, eastern Poland) where ice wedging is bracketed between ca. 30 and ca. 25 ka, two intervals of very harsh periglacial climate are identified in the studied sections. Whereas the latter coincides with the lower MIS 2 (beginning of the Upper Pleniglacial), the ice wedging at Zaprężyn most probably occurred during MIS 4. This corresponds to the presumably oldest ice wedge network and associated permafrost evidence for the last glacial in Poland but also in western central Europe (see Nussloch TK 2 before the lowest Gräselberg soil; Antoine et al., 2015). The overlying loess below the discordance in the Zaprężyn section with periglacial habitus (but without ice wedging) yields quartz ages around 50 to 57 ka, which argue for lower MIS 3. We hypothesize that this periglacial loess reflects the Ristinge ice advance (50–55 ka) in the southwestern Baltic Sea area. But attribution of luminescence ages to certain MISs is not yet always unambiguous. An analogue control by the Klintholm ice advance (30–34 ka) may be discussed for the loess of the upper L1SS1 pedocomplex at the Złota section (ZL-3, ca. 32 ka). The actual database is, however, too sparse to prove these hypotheses, and the discussed problems of optical dating need more clearness.

In spite of the addressed uncertainties, we can so far for honesty reasons recommend aiming at age bracketing as narrowly as possible, using OSL from different quartz fractions and pIRIR from fine polymineral grains. In the case of the L1SS1 pedocomplex, for example, age bracketing between ca. 30 and 40 ka demonstrates the helpfulness of this approach. Exact dating remains challenging, in particular for a periglacial environment with strong heterogeneity of the dated material (Fig. S2).

Data availability. Relevant data are given in the Supplement, in particular in Table S1 “Analytical data and ages”.

Supplement. The supplement related to this article is available online at: https://doi.org/10.5194/egqsj-71-59-2022-supplement.

Author contributions. LZ drafted the manuscript, conducted fieldwork and sampling, designed several figures, completed the check of luminescence dating results, and calculated final ages. MF undertook laboratory work including evaluation of luminescence measurements and the first calculation of ages. ZJ conducted fieldwork and sampling, designed several figures, was involved in continual discussions with all authors, and made fundamental contributions to the manuscript. PA conducted fieldwork and sampling at two sites, designed Figs. 8 and 10a, and contributed to the manuscript. MK conducted fieldwork and sampling, designed and finalized several figures, and gave a detailed description of profiles.

Competing interests. The contact author has declared that neither they nor their co-authors have any competing interests.

Disclaimer. Publisher’s note: Copernicus Publications remains neutral with regard to jurisdictional claims in published maps and institutional affiliations.

Acknowledgements. The research results were sponsored by the German Science Foundation DFG, project number ZO51/39-1, “Harsh periglacial climate at MIS 3/MIS 2 transition reflected in Central European Loess-Paleosol Sequences”, and by the National

Science Centre, Poland, project no. 2017/27/B/ST10/01854 entitled "Sudden COLD events of the Last Glacial in the central part of the European LOESS Belt – in Poland and in the western part of Ukraine (COLD LOESS)".

The authors thank the two anonymous reviewers for helpful remarks to improve the manuscript.

Financial support. This research has been supported by the Deutsche Forschungsgemeinschaft (grant no. ZO51/39-1) and the National Science Centre, Poland (grant no. 2017/27/B/ST10/01854).

This open-access publication was funded by the University of Bayreuth.

Review statement. This paper was edited by Tony Reimann and reviewed by two anonymous referees.

References

Aitken, M. J.: An introduction to optical dating, 267 pp., University Press, Oxford, ISBN 0198540922 (Hbk), 1998.

Antoine, P.: Thermokarst processes and features from west-European loess series: new evidences for rapid climatic warming events during the Last Glacial, Quatern. Int., 21, 279–280, https://doi.org/10.1016/j.quaint.2012.07.088, 2013.

Antoine, P., Goval, E., Jamet, G., Coutard, S., Moine, O., Herisson, D., Auguste, P., Guerin, G., Lagroix, F., Schmidt, E., Robert, V., Debenham, N., Meszner, S., and Bahain, J.-J.: Les séquences loessiques pléistocène supérieur d'Havrincourt (Pas-de-Calais, France): stratigraphie, paléoenvironnement, géochronologie et occupations paléolithiques, Quaternaire, 25, 321–368, https://doi.org/10.4000/quaternaire.7278, 2014.

Antoine, P., Coutard, S., Guerin, G., Deschodt, L., Goval, E., and Locht, J.-L.: Upper Pleistocene loess-palaeosol records from northern France in the European context: environmental background and dating of the Middle Palaeolithic, Quatern. Int., 411, 4–24, https://doi.org/10.1016/j.quaint.2015.11.036, 2015.

Avram, A., Constantin, D., Veres, D., Kelemen, S., Obreht, I., Hambach, U., Markovic, S. B., and Timar-Gabor, A.: Testing polymineral post-IR IRSL and quartz SAR-OSL protocols on Middle to Late Pleistocene loess at Batajnica, Serbia, Boreas, 49, 615–633, https://doi.org/10.1111/bor.12442, 2020.

Badura, J., Jary, Z., and Smalley, I.: Sources of loess material for deposits in Poland and parts of Central Europe: the lost big river, Quatern. Int., 296, 15–22, https://doi.org/10.1016/j.quaint.2012.06.019, 2013.

Butrym, J. and Maruszczak, H.: Thermoluminescence chronology of loesses at Nieledew profile, Scientific Research Report of Committee of Quaternary Research of the Polish Academy of Science 3, 1983 (in Polish).

Chapot, M. S., Roberts, H. M., Duller, G. A. T., and Lai, Z. P.: A comparison of natural- and laboratory-generated dose response curves for quartz optically stimulated luminescence signals from Chinese Loess, Radiat. Meas., 47, 1045–1052, 2012.

Degering, D. and Degering, A: Change is the only constant – time-dependent dose rates in luminescence dating, Quat. Geochronol., 58, 101074, https://doi.org/10.1016/j.quageo.2020.101074, 2020.

Duller, G. A. T.: The Analyst software package for luminescence data: overview and recent improvements, Ancient TL, 33, 35–42, 2015.

Fitzsimmons, K. E. and Hambach, U.: Loess accumulation during the last glacial maximum: Evidence from Urluia, southeastern Romania, Quatern. Int., 334–335, 74–85, https://doi.org/10.1016/j.quaint.2013.08.005, 2013.

Fuchs, M., Kreutzer, S., Rousseau, D. D., Antoine, P., Hatté, C., Lagroix, F., Moine, O., Gauthier, C., Svoboda, J., and Lisá, L.: The loess sequence of Dolní Věstonice, Czech Republic: A new OSL-based chronology of the Last Climatic Cycle, Boreas, 42, 664–677, https://doi.org/10.1111/j.1502-3885.2012.00299.x, 2013.

Gocke, M., Kuzyakov, Y., and Wiesenberg, G. L. B.: Rhizoliths in loess – evidence for post-sedimentary incorporation of root-derived organic matter in terrestrial sediments as assessed from molecular proxieset, Org. Geochem., 41, 1198–1206, https://doi.org/10.1016/j.orggeochem.2010.08.001, 2010.

Guérin, G., Mercier, N., and Adamiec, G.: Dose-rate conversion factors: update, Ancient TL, 29, 5–8, 2011.

Haase, D., Fink, J., Haase, G., Ruske, R., Pécsi, M., Richter, H., Altermann, M., and Jäger, K.-D.: Loess in Europe – its spatial distribution based on a European loess map, scale 1 : 2 500 000, Quaternary Sci. Rev. 26, 1301–1312, https://doi.org/10.1016/j.quascirev.2007.02.003, 2007.

Hardt, J., Lüthgens, C., Hebenstreit, R., and Böse, M.: Geochronological (OSL) and geomorphological investigations at the presumed Frankfurt ice marginal position in northeast Germany, Quaternary Sci. Rev., 154, 85–99, https://doi.org/10.1016/j.quascirev.2016.10.015, 2016.

Hughes, P. D., Gibbard, P. L., and Ehlers, J.: Timing of glaciation during the last glacial cycle: evaluating the concept of a global "Last Glacial Maximum" (LGM), Earth-Sci. Rev., 125, 171–198, https://doi.org/10.1016/j.earscirev.2013.07.003, 2013.

Jary, Z.: Record of climate changes in Upper Pleistocene loess-soil sequences in Poland and western part of Ukraine, Rozprawy Naukowe Instytutu Geografii i Rozwoju Regionalnego Uniwersytetu Wrocławskiego 1, 136 pp., Wrocław, ISBN 83-921524-5-X, 2007 (in Polish, with English abstract).

Jary, Z.: Periglacial markers within the Late Pleistocene loess-palaeosol sequences in Poland and western Ukraine, Quatern. Int., 198, 124–135, https://doi.org/10.1016/j.quaint.2008.01.008, 2009.

Jary, Z. (Ed.): Closing the gap – North Carpathian loess travers in the Eurasian loess belt, International Workshop, 6th Loess Seminar in Wrocław, Poland, 16–21 May 2011, Abstract and field guide book, Institute of Geography and Regional Development, University of Wrocław, ISBN 978-83-62673-06-3, 2011.

Jary, Z. and Ciszek, D.: Late Pleistocene loess-palaeosol sequences in Poland and western Ukraine, Quatern. Int., 296, 37–50, https://doi.org/10.1016/j.quaint.2012.07.009, 2013.

Jary, Z. and Krzyszkowski, D.: Stratigraphy, properties and origin of loess in Trzebnica Brickyard, southwestern Poland, Acta Universitatis Wratislaviensis No. 1702, Prace Instytutu Geograficznego, Seria A, Geografia Fizyczna VII, 63–83, ISBN 83-229-1228-5, 1994.

Jary, Z., Ciszek, D., Kida, J., Karamański, P., and Raczyk, J: Late Pleistocene loess-soil sequence in Zaprężyn, edited by: Jary, Z., Closing the gap – North Carpathian loess traverse in the Eurasian loess belt, International Workshop, 6th Loess Seminar, Wrocław, Poland, 16–21 May 2011, Abstract and field guide book, Institute of Geography and Regional Development, University of Wrocław, 51–52, ISBN 978-83-62673-06-3, 2011.

Kreutzer, S., Fuchs, M., Meszner, S., and Faust, D.: OSL chronostratigraphy of a loess-palaeosol sequence in Saxony/Germany using quartz of different grain sizes, Quat. Geochronol. 10, 102–109, https://doi.org/10.1016/j.quageo.2012.01.004, 2012.

Kreutzer, S., Schmidt, C., DeWitt, R., and Fuchs, M., The a-value of polymineral fine grain samples measured with the post-IR IRSL protocol, Radiat. Meas., 69, 18–29, 2014.

Krzyszkowski, D.: The Wartanian Siedlec Sandur (Zedlitzer Sandur) southwards the Trzebnica Hills, Silesian Lowland; Southwestern Poland: re-examination after fifty years, E&G Quaternary Sci. J., 43, 53–66, https://doi.org/10.3285/eg.43.1.05, 1993.

Lai, Z. P., Zöller, L., Fuchs, M., and Brückner, H.: Alpha efficiency determination for OSL of quartz extracted from Chinese loess, Radiat. Meas., 43, 767–770, https://doi.org/10.1016/j.radmeas.2008.01.022, 2008.

Léger, M.: Loess landforms, Quatern. Int., 7/8, 53–61, 1990.

Lowick, S. E. and Preusser, F.: Investigating age underestimation in the high dose region of optically stimulated luminescence using fine grain quartz, Quat. Geochronol., 6, 33–41, 2011.

Lüthgens, C. and Böse, M.: Chronology of Weichselian main ice marginal positions in north-eastern Germany, E&G Quaternary Sci. J., 60, 17, https://doi.org/10.3285/eg.60.2-3.02, 2011.

Lüthgens, C., Hardt, J., and Böse, M.: Proposing a new conceptual model for the reconstruction of ice dynamics in the SW sector of the Scandinavian Ice Sheet (SIS) based on the reinterpretation of published data and new evidence from optically stimulated luminescence (OSL) dating, E&G Quaternary Sci. J., 69, 201–223, https://doi.org/10.5194/egqsj-69-201-2020, 2020.

Marković, S. B., Stevens, T., Kukla, G. J., Hambach, U., Fitzsimmons, K. E., Gibbard, P., Buggle, B., Zech, M., Guo, Z., Hao, Q., Wu, H., O'Hara-Dhand, K., Smalley, I. J., Ujvari, G., Sumegi, P., Timar-Gabor, A., Veres, D., Sirocko, F., Vasiljević, D. A., Jary, Z., Svensson, A., Jović, V., Lehmkuhl, F., Kovacs, J., and Svircev, Z.: Danube loess stratigraphy – Towards a pan-European loess stratigraphic model, Earth Sci. Rev., 148, 228–258, https://doi.org/10.1016/j.earscirev.2015.06.005, 2015.

Marks, L.: Pleistocene glacial limits in the territory of Poland, Przegląd Geologiczny, 53, 988–993, 2005.

Marks, L.: Quaternary Glaciations in Poland, in: Developments in Quaternary Science, edited by: Ehlers, J., Gibbard, P. L., and Hughes, P. D., Amsterdam, the Netherlands, vol. 15, 299–303, ISBN 9780444534477, 2011.

Maruszczak, H.: Zróżnicowanie stratygraficzne lessów polskich (Stratigraphical differentiation of Polish loesses), 1991, in: Podstawowe profile lessów w Polsce (Main section of loesses in Poland), edited by: Maruszczak, H., Wyd. UMCS, Lublin, A, 13–35, ISBN 83-227-0388-0, 1991.

Maruszczak, H.: Schemat stratygrafii lessów i gleb śródlessowych w Polsce (Stratigraphic scheme of loesses and paleosols in Poland), in: Podstawowe profile lessów w Polsce II (Main section of loesses in Poland II), edited by: Maruszczak, H., Wyd. UMCS, Lublin, 17–29, ISBN 83-227-1723-7, 2001.

Meszner, S., Kreutzer, S., Fuchs, M., and Faust, D.: Late Pleistocene landscape dynamics in Saxony, Germany: Paleoenvironmental reconstruction using loess-paleosol sequences, Quatern. Int. 296, 94–107, https://doi.org/10.1016/j.quaint.2012.12.040, 2013.

Moine, O., Antoine, P., Hatté, C., Landais, A., Mathieu, J., Prud'homme, C., and Rousseau, D.-D.: The impact of Last Glacial climate variability in west-European loess revealed by radiocarbon dating of fossil earthworm granules, P. Natl. Acad. Sci. USA, 114, 6209–6214, https://doi.org/10.1073/pnas.1614751114, 2017.

Moska, P. and Bluszcz, A.: Luminescence dating of loess profiles in Poland, Quatern. Int., 296, 51–60, https://doi.org/10.1016/j.quaint.2012.09.004, 2013.

Moska, P., Adamiec, G., and Jary, Z.: OSL dating and lithological characteristics of loess deposits from Biały Kościół, Geochronometria, 38, 162–171, https://doi.org/10.2478/s13386-011-0013-x, 2011.

Moska, P., Adamiec, G., and Jary, Z.: High resolution dating of loess profile from Biały Kościół, southwest Poland, Quat. Geochronol., 10, 87–93, https://doi.org/10.1016/j.quageo.2012.04.003, 2012.

Moska, P., Jary, Z., Adamiec, G., and Bluszcz, A.: OSL chronostratigraphy of a loess-paleosol sequence in Złota using quartz and polymineral fine grains, Radiat. Meas., 81, 23–31, https://doi.org/10.1016/j.radmeas.2015.04.012, 2015.

Moska, P., Adamiec, G., Jary, Z., and Bluszcz, A.: OSL chronostratigraphy for loess deposits from Tyszowce – Poland, Geochronometria, 44, 307–318, https://doi.org/10.1515/geochr-2015-0074, 2017.

Moska, P., Adamiec Jary, Z. G., Bluszcz, A., Poręba, G., Piotrowska, N., Krawczyk, M., and Skurzyński, J.: Luminescence chronostratigraphy for the loess deposits in Złota, Poland, Geochronometria, 45, 44–55, 2018.

Moska, P., Jary, Z., Adamiec, G., and Bluszcz, A.: Chronostratigraphy of a loess-palaeosol sequence in Biały Kościół, Poland using OSL and radiocarbon dating, Quatern. Int., 502, 4–17, https://doi.org/10.1016/j.quaint.2018.05.024, 2019.

Murray, A. S. and Wintle, A. G.: Luminescence dating of quartz using an improved single aliquot regenerative-dose protocol, Radiat. Meas., 32, 57–73, 2000.

Murray, A. S., Schmidt, E. D., Stevens, T. Buylaert, J.-P., Marković, S. B., Tsukamoto, S., and Frechen, M.: Dating Middle Pleistocene loess from Stari Slankamen (Vojvodina, Serbia) – Limitations imposed by the saturation behaviour of an elevated temperature IRSL signal, Catena, 117, 34–42, https://doi.org/10.1016/j.catena.2013.06.029, 2013.

Murton, J. B.: Thermokarst sediments and sedimentary structures, Tuktoyaktuk Coastlands, western Arctic Canada, Global Planet. Change, 28, 175–192, 2001.

Preusser, F., Degering, D., Fuchs, M., Hilgers, A., Kadereit, A., Klasen, N., Krbetschek, M., Richter, D., and Spencer, J. Q. G.: Luminescence dating: basics, methods and applications, E&G Quaternary Sci. J., 57, 95–149, https://doi.org/10.3285/eg.57.1-2.5, 2008.

Rousseau, D.-D., Boers, N., Sima, A., Svensson, A., Bigler, M., Lagroix, F., Taylor, S., and Antoine, P.: (MIS3 & 2) millennial oscillations in Greenland dust and Eurasian aeolian records – A paleosol perspective, Quaternary Sci. Rev., 169, 99–113, https://doi.org/10.1016/j.quascirev.2017.05.020, 2017.

Różycki, S. Z.: Le sens des vents portant la poussiere de loess a la lumiere de l'analyse des formes d'accumulation du loess en Bulgarie et en Europe Centrale, Revue de geomorphologie dynamique, 1, 1–9, 1967.

Scheidt, S., Berg, S., Hambach, U., Klasen, N., Pötter, S., Stolz, A., Veres, D., Zeeden, C., Brill, D., Brückner, H., Kusch, S., Laag, C., Lehmkuhl, F., Melles, M., Monnens, F., Oppermann, L., Rethemeyer, J., and Nett, J. J.: Chronological assessment of the Balta Alba Kurgan loess-paleosol section (Romania) – a comparative study on different dating methods for a robust and precise age model, Front. Earth Sci., 8, 598448, https://doi.org/10.3389/feart.2020.598448, 2021.

Schmidt, C., Bösken, J., and Kolb, T.: Is there a common alpha-efficiency in polymineral samples measured by various infrared stimulated luminescence protocols?, Geochronometria, 45, 160–172, 2018.

Schmidt, C., Zeeden, C., Krauß, L., Lehmkuhl, F., and Zöller, L.: A chronological and palaeoenvironmental re-evaluation of two loess-palaeosol records in the northern Harz foreland (Germany) based on innovative modelling tools, Boreas, 50, 746–763, https://doi.org/10.1111/bor.12510, 2021.

Thiel, C., Buylaert, J.-P., Murray, A. S., Terhorst, B., Tsukamoto, S., Frechen, M., and Sprafke, T.: Investigating the chronostratigraphy of prominent palaeosols in Lower Austria using post-IR IRSL dating, E&G Quaternary Sci. J., 60, 11, https://doi.org/10.3285/eg.60.1.10, 2011.

Timar-Gabor, A. and Wintle, A. G.: On natural and laboratory generated dose response curves for quartz of different grain sizes from Romanian loess, Quat. Geochronol., 18, 34–40, 2013.

Timar-Gabor, A., Constantin, D., Buylaert, J. P., Jain, M., Murray, A. S., and Wintle, A. G.: Fundamental investigations of natural and laboratory generated SAR dose response curves for quartz OSL in the high dose range, Radiat. Meas., 81, 150–156, 2015.

Timar-Gabor, A., Buylaert, J.-P., Guralnik, B., Trandafir-Antohi, O., Constantin, D., Anachitei-Deacu, V., Jain, M., Murray, A. S., Porat, N., Hao, Q., and Wintle, A. G.: On the importance of grain size in luminescence dating using quartz, Radiat. Meas., 106, 464–471, https://doi.org/10.1016/j.radmeas.2017.01.009, 2017.

Waroszewski, J., Pietranik, A., Sprafke, T., Kabała, C., Frechen, M., Jary, Z., Kot, A., Tsukamoto, S., Meyer-Heintze, S., Krawczyk, M., Łabaz, B., Schultz, B., and Erban Kochergina, Y. V.: Provenance and paleoenvironmental context of the Late Pleistocene thin aeolian silt mantles in southwestern Poland. A widespread parent material for soils, Catena, 204, 105377, https://doi.org/10.1016/j.catena.2021.105377, 2021.

Wolf, D., Kolb, T., Alcaraz-Castaño, M., Heinrich, S., Baumgart, P., Calvo, R., Sánchez, J., Ryborz, K., Schäfer, I., Bliedtner, M., Zech, R., Zöller, L., and Faust, D.: Climate deteriorations and Neanderthal demise in interior Iberia, Sci. Rep., 8, 7048, https://doi.org/10.1038/s41598-018-25343-6, 2018.

Zöller, L.: Geomorphologische und geologische Interpretation von Thermolumineszenz-Daten, Bayreuther Geowissenschaftliche Arbeiten, 14, 103–112, 1989.

Zöller, L. and Pernicka, E.: A note on overcounting in alpha-counters and its elimination, Ancient TL, 7, 11–14, 1989.

Zöller, L., Richter, D., Blanchard, H., Einwögerer, T., Händel, M., and Neugebauer-Maresch, C.: Our oldest children: Age constraints for the Krems-Wachtberg site obtained from various thermoluminescence dating approaches, Quatern. Int., 351, 83–87, https://doi.org/10.1016/j.quaint.2013.05.003, 2014.